Electronic supplementary information

Synthesis and characterization of aminopyridine iron(II) chloride catalysts for isoprene polymerization: sterically controlled monomer enchainment

Chuyang Jing,[1,2†] Liang Wang,[1†] Qaiser Mahmood,[1] Mengmeng Zhao,[1] Guangqian Zhu,[1,2] Xianhui Zhang,[1,2] Xiaowu Wang,[1*], Qinggang Wang[1*]

[1]Key Laboratory of Biobased Materials, Qingdao Institute of Bioenergy and Bioprocess Technology, Chinese Academy of Sciences, Qingdao, 266101, China.

[2]Center of Materials Science and Optoelectronics Engineering, University of Chinese Academy of Sciences, Beijing, 100049, China.

Correspondence: E-mail: wangqg@qibebt.ac.cn; wangxw@qibebt.ac.cn)

1. Isoprene Polymerization Using $Fe8_H$–$Fe10_H$ /MAO [a]

Entry	Cat.	Yield %	Act. [b]	Microstructure(%) [c]		
				cis-1,4	*trans*-1,4	3,4-
1	$Fe8_H$	>99	81.6	33	19	48
2	$Fe9_H$	>99	81.6	31	20	49
3	$Fe10_H$	>99	81.6	40	10	50

[a] Polymerization conditions: solvent: 5 mL toluene; complex: 10 µmol; isoprene: 20 mmol; time: 10 min; T: 25 °C; MAO/Fe: 500; [b] 10^4 g·mol^{-1}·h^{-1}; [c] determined by ^{1}H NMR and ^{13}C NMR;

2. Synthesis of the pyridine-amide iron complex and its catalysis toward isoprene polymerization

2.1 Synthesis of the pyridine-amide iron complex

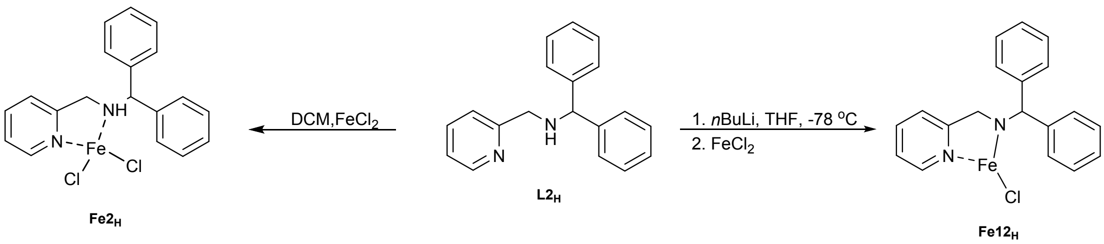

2.2 Isoprene Polymerization Using $Fe12_H$/MAO [a]

Entry	Cat.	Yield %	Act. [b]	Microstructure(%) [c]		
				cis-1,4	*trans*-1,4	3,4-
1	$Fe12_H$	>99	6.8	50	--	50

[a] Polymerization conditions: solvent: 5 mL toluene; complex: 10 µmol; isoprene: 20 mmol; time: 2 h; T: 25 °C; MAO/Fe: 500; [b] 10^4 g·mol^{-1}·h^{-1}; [c] determined by ^{1}H NMR and ^{13}C NMR;

2. NMR Spectra of the Ligands

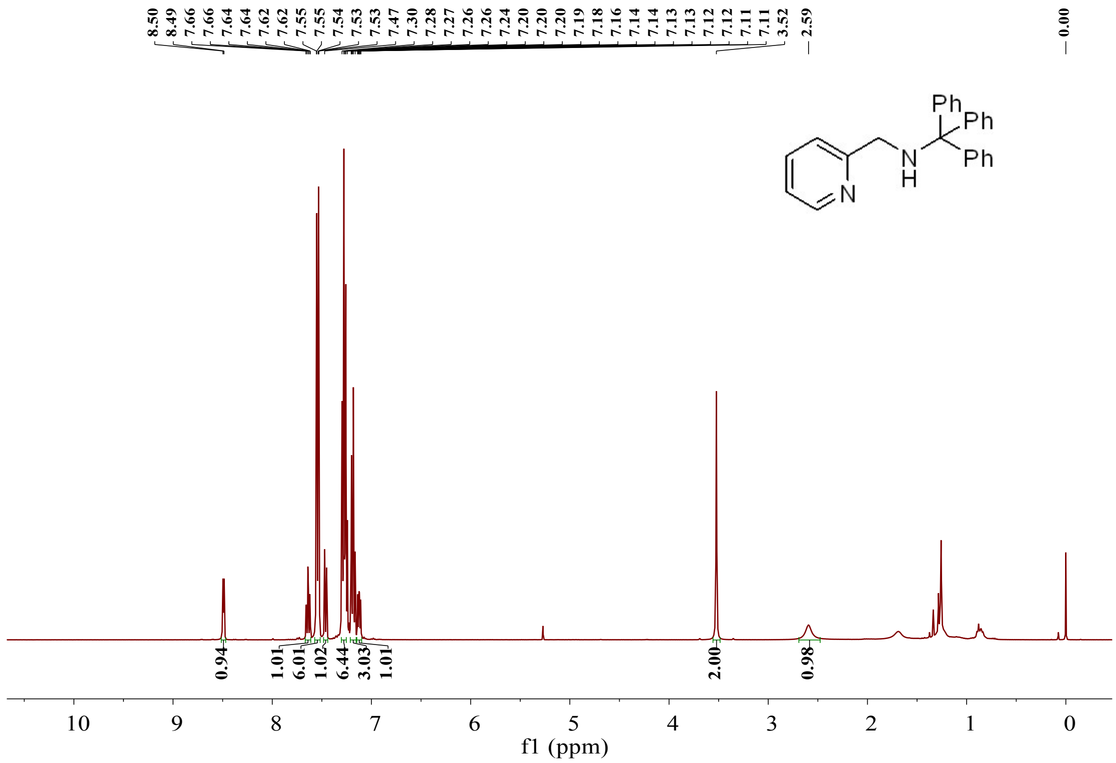

Figure S1. ^{1}H NMR spectrum (400 MHz, $CDCl_3$, 298 K) of $L1_H$

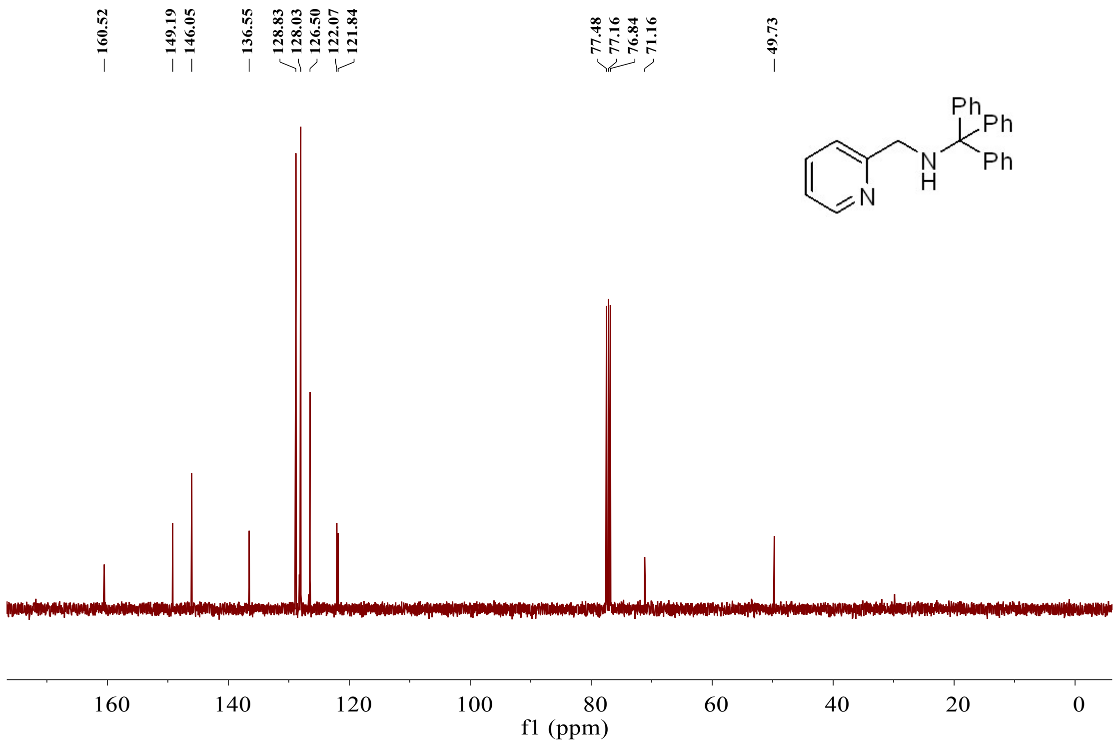

Figure S2. ^{13}C NMR spectrum (100 MHz, $CDCl_3$, 298 K) of $L1_H$

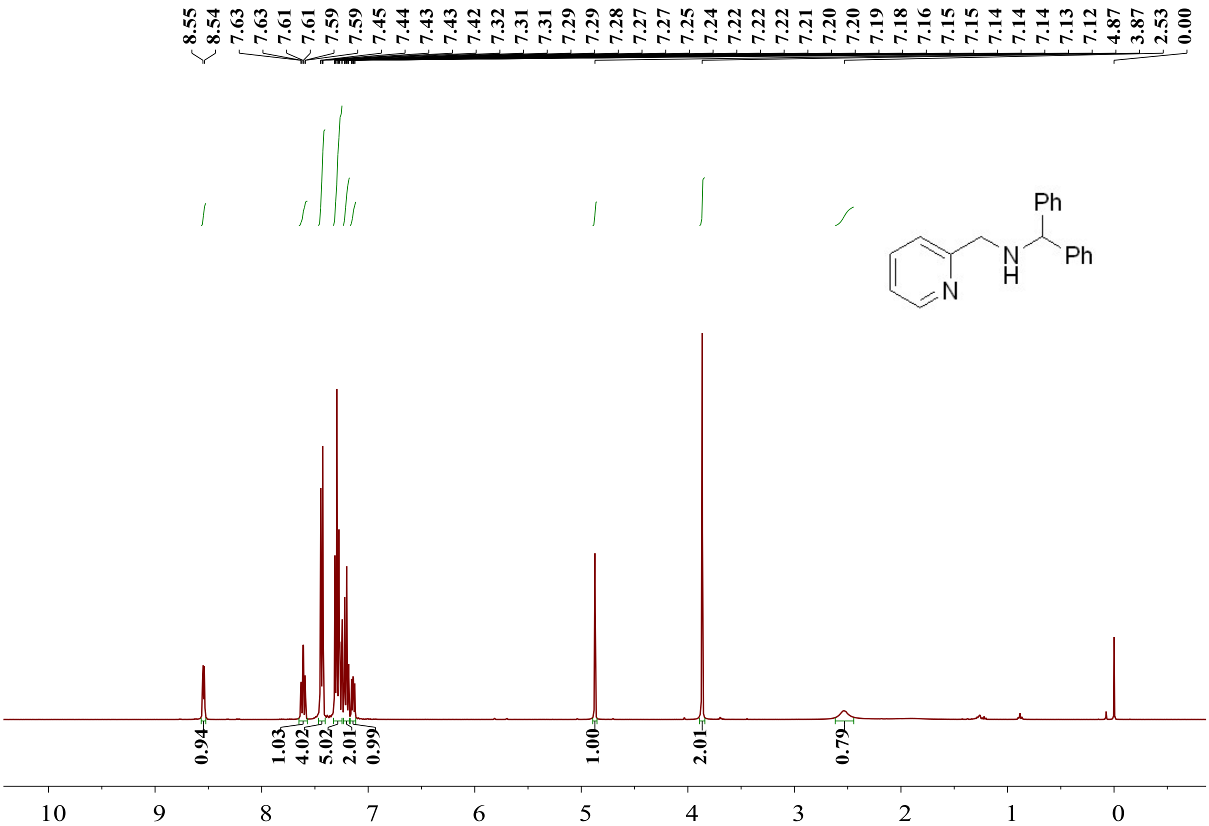

Figure S3. ^{1}H NMR spectrum (400 MHz, $CDCl_3$, 298 K) of $L2_H$

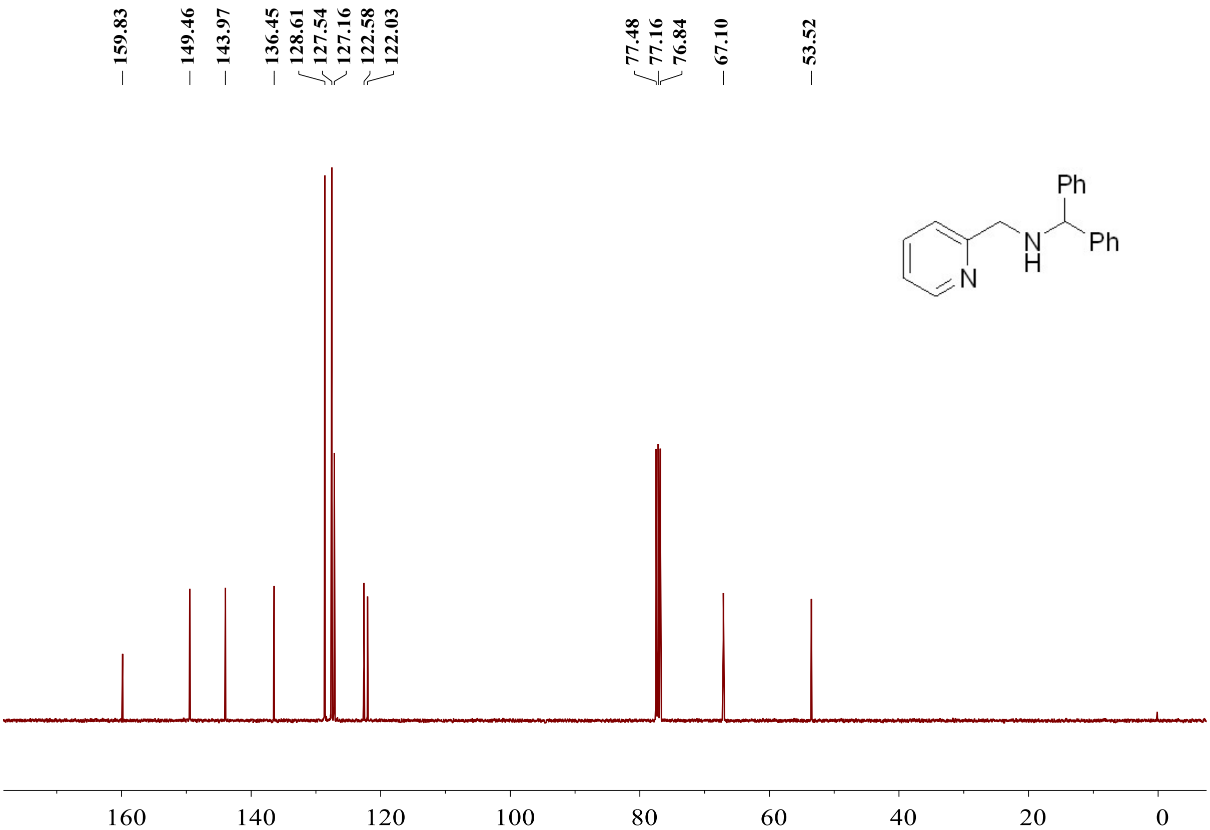

Figure S4. ^{13}C NMR spectrum (100 MHz, $CDCl_3$, 298 K) of $L2_H$

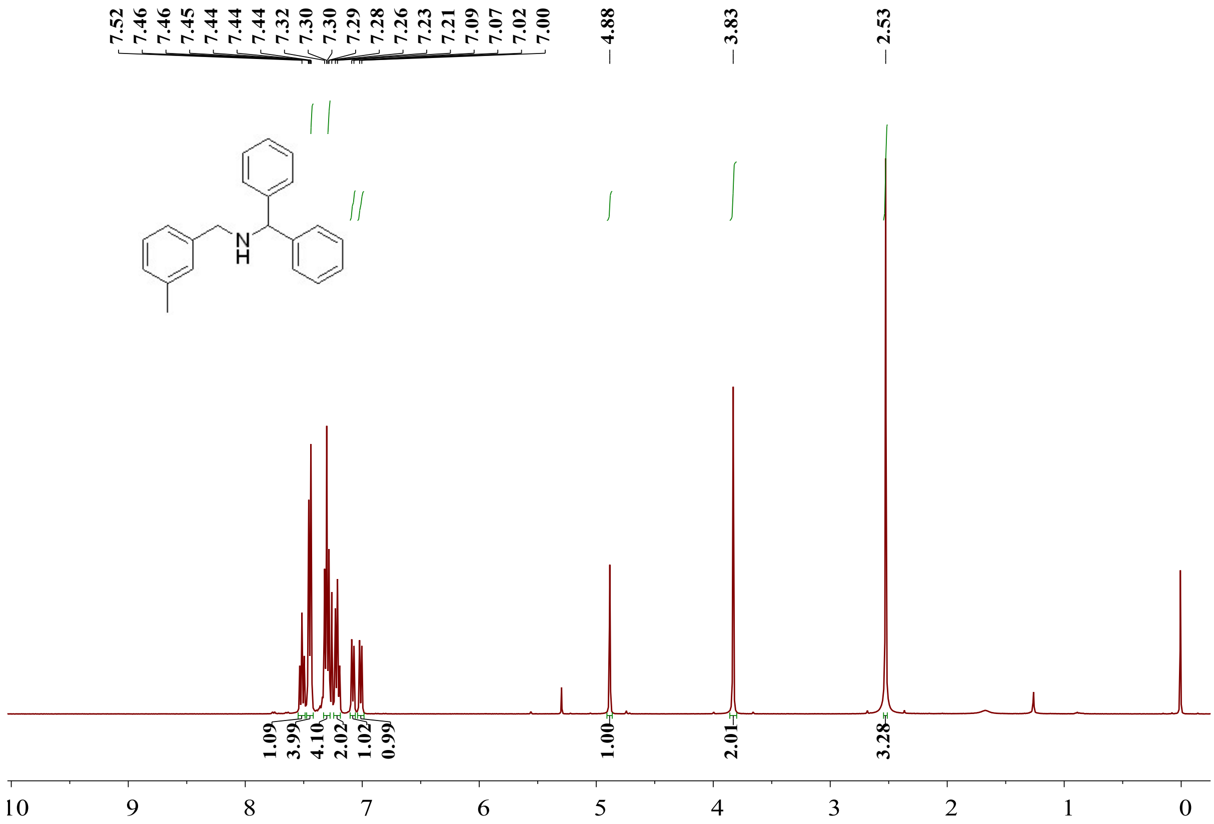

Figure S5. ^{1}H NMR spectrum (400 MHz, $CDCl_3$, 298 K) of $L3_{Me}$

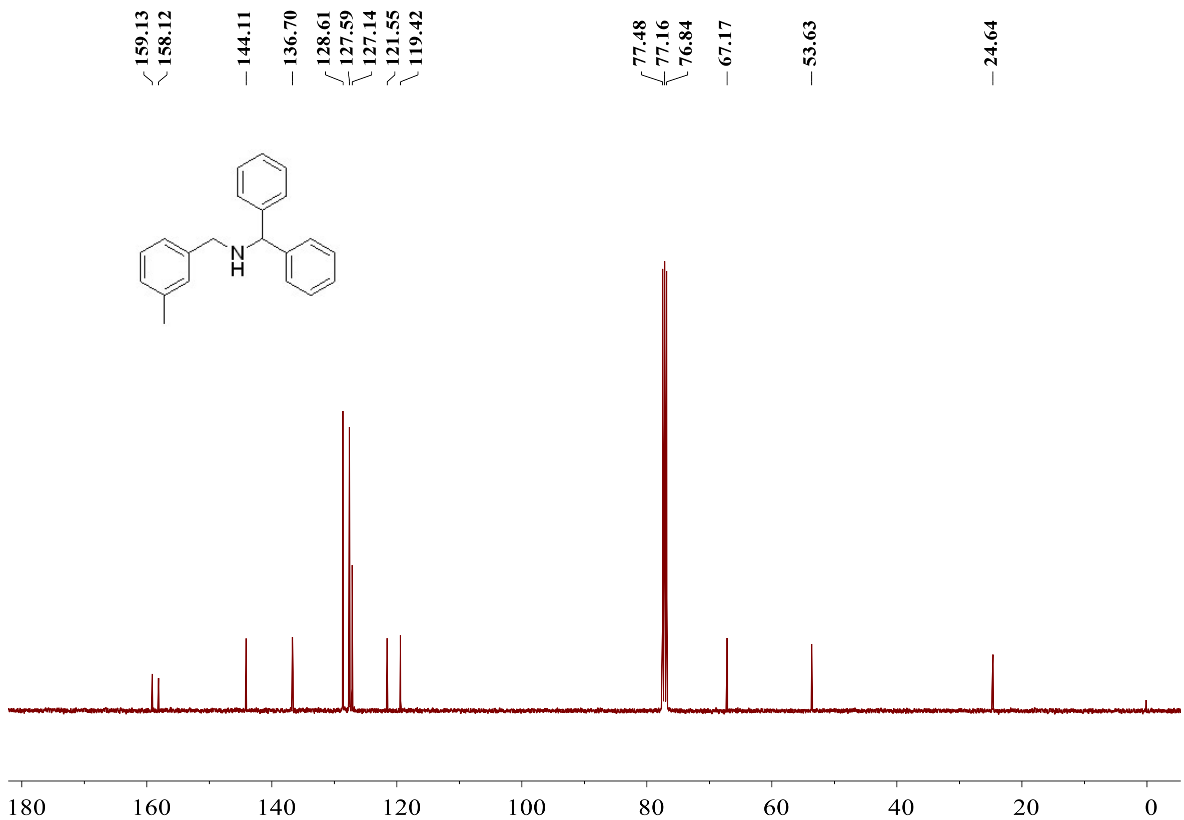

Figure S6. ^{13}C NMR spectrum (100 MHz, $CDCl_3$, 298 K) of $L3_{Me}$

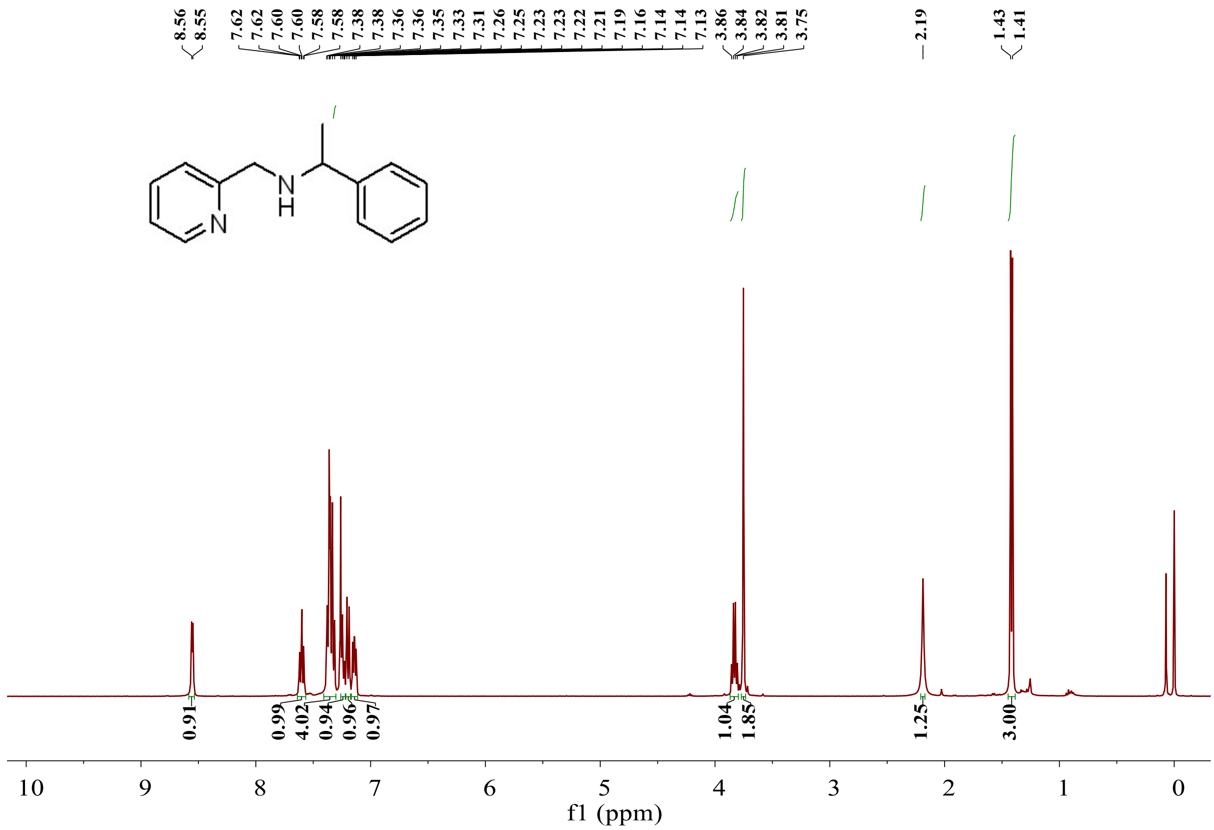

Figure S7. ^{1}H NMR spectrum (400 MHz, $CDCl_3$, 298 K) of $L4_H$

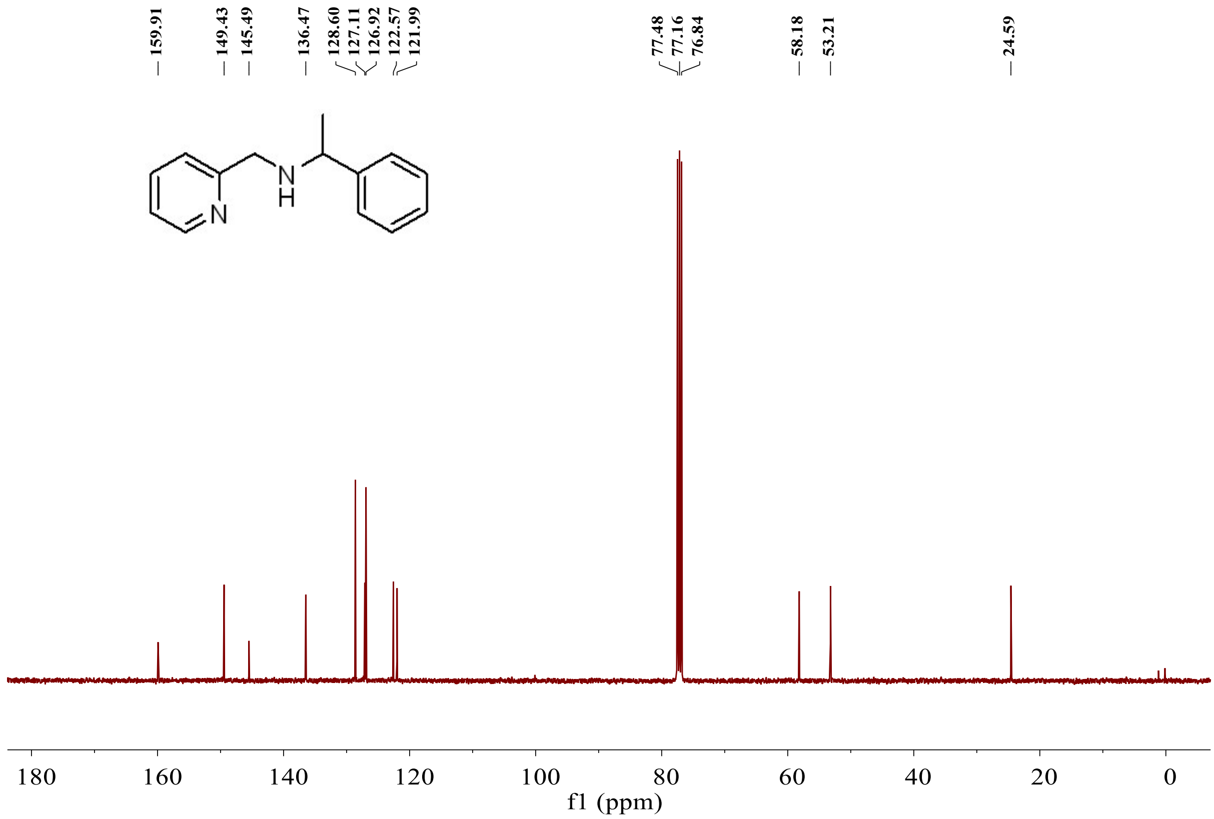

Figure S8. ^{13}C NMR spectrum (100 MHz, $CDCl_3$, 298 K) of $L4_H$

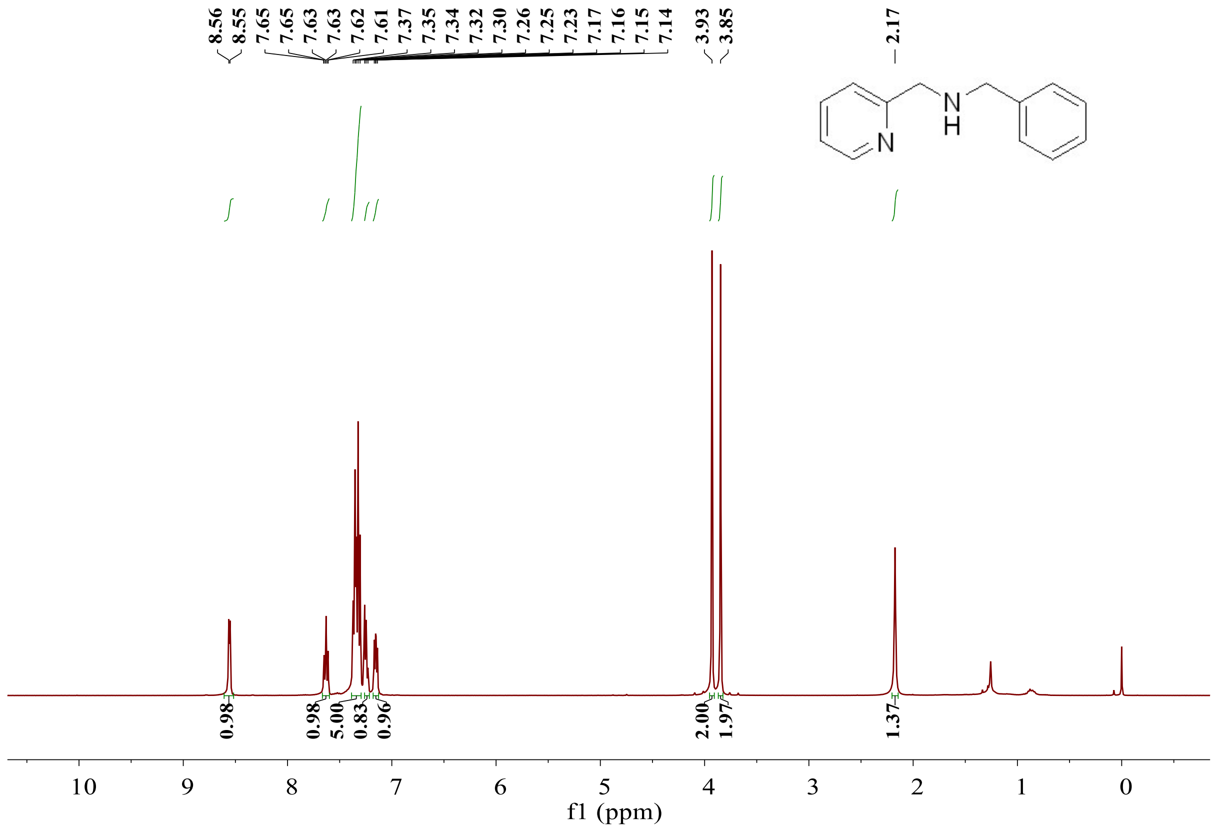

Figure S9. ^{1}H NMR spectrum (400 MHz, $CDCl_3$, 298 K) of $L5_H$

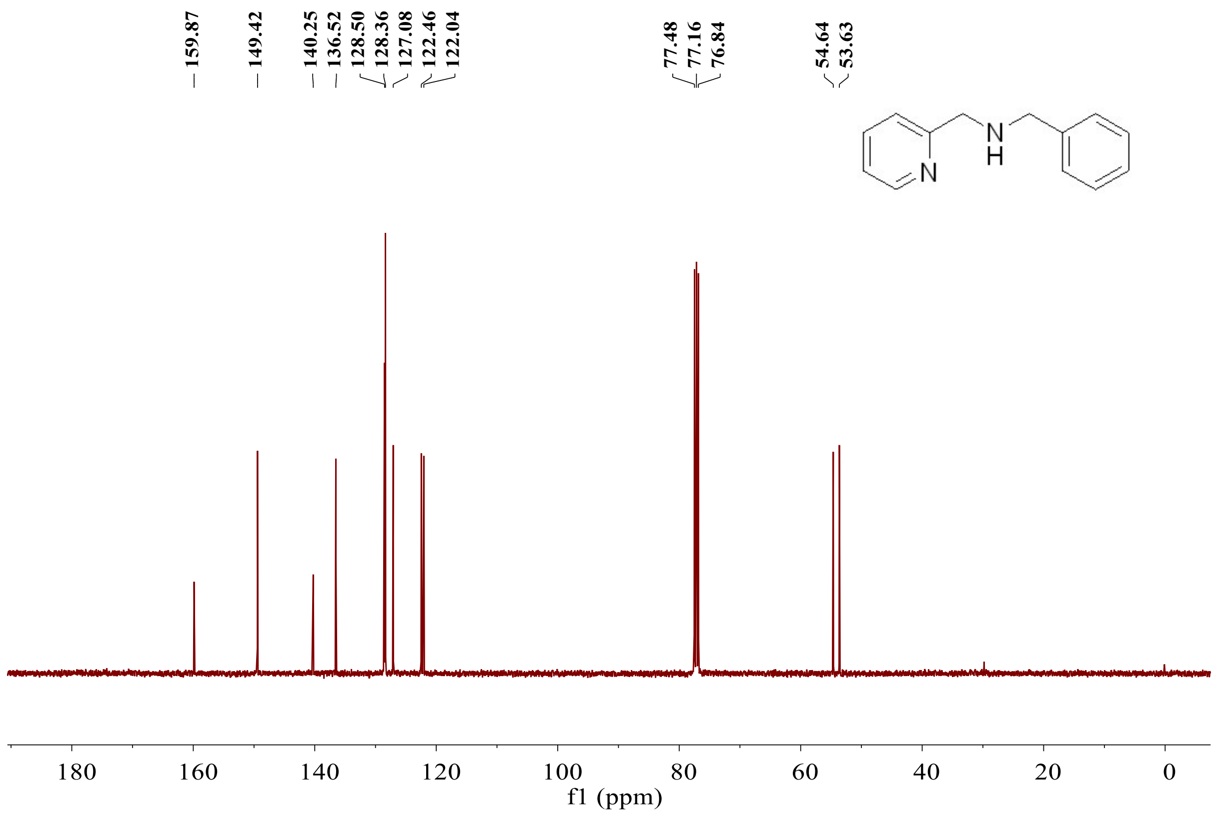

Figure S10. ^{13}C NMR spectrum (100 MHz, $CDCl_3$, 298 K) of $L5_H$

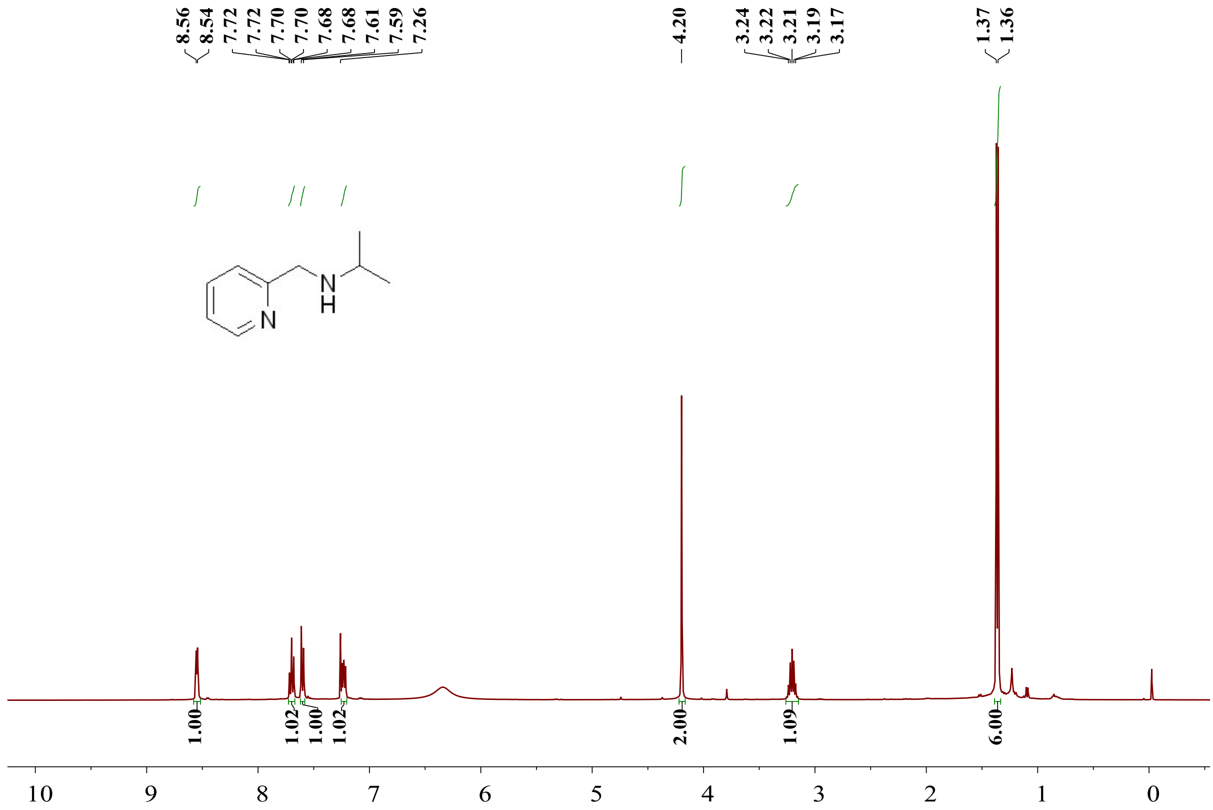

Figure S11. ^{1}H NMR spectrum (400 MHz, $CDCl_3$, 298 K) of $L6_H$

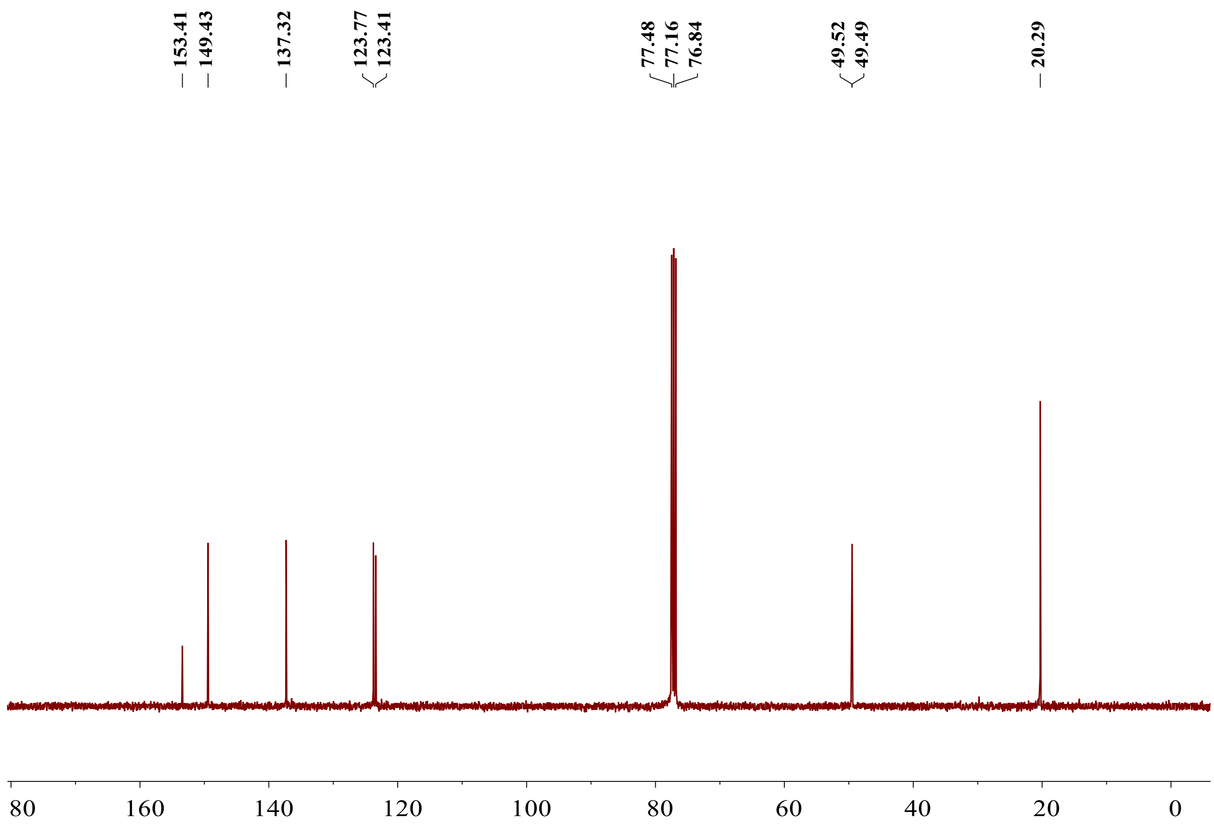

Figure S12. ^{13}C NMR spectrum (100 MHz, $CDCl_3$, 298 K) of $L6_H$

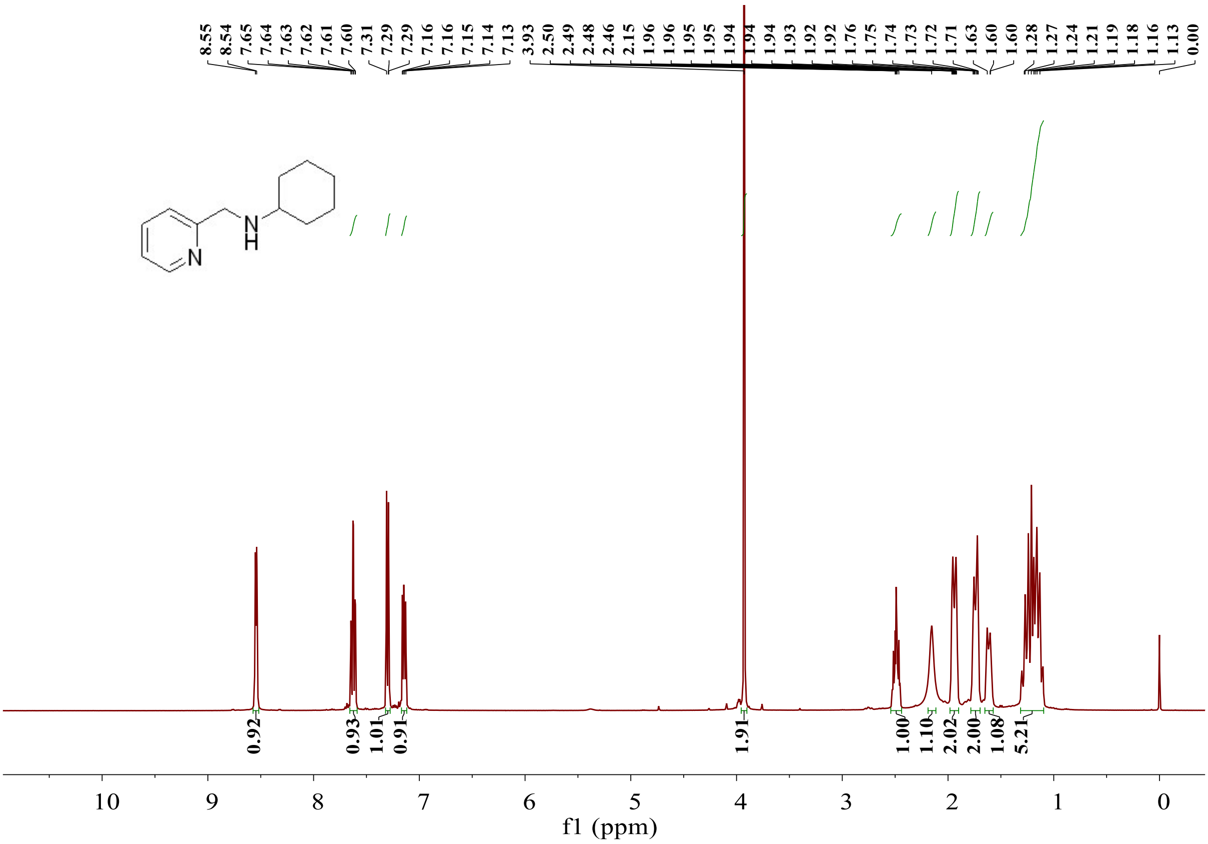

Figure S13. ^{1}H NMR spectrum (400 MHz, $CDCl_3$, 298 K) of $L7_H$

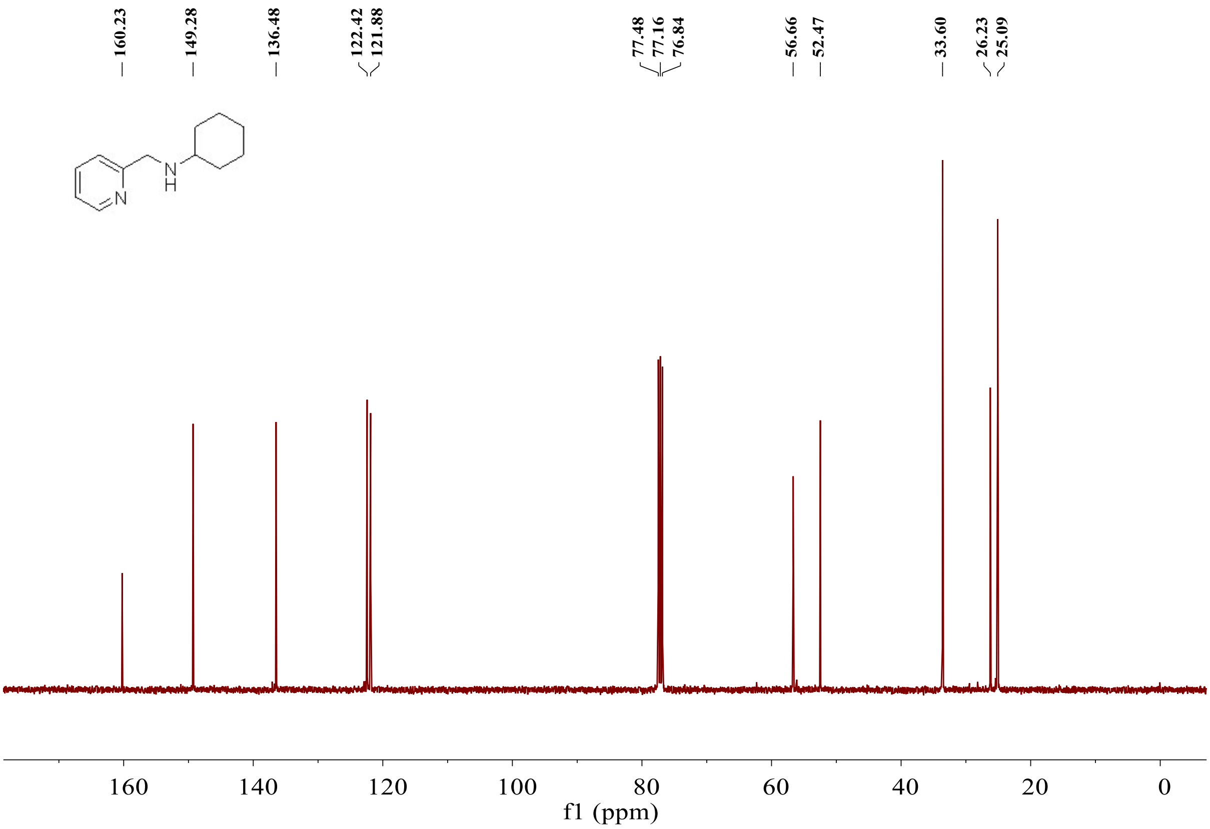

Figure S14. ^{13}C NMR spectrum (100 MHz, $CDCl_3$, 298 K) of $L7_H$

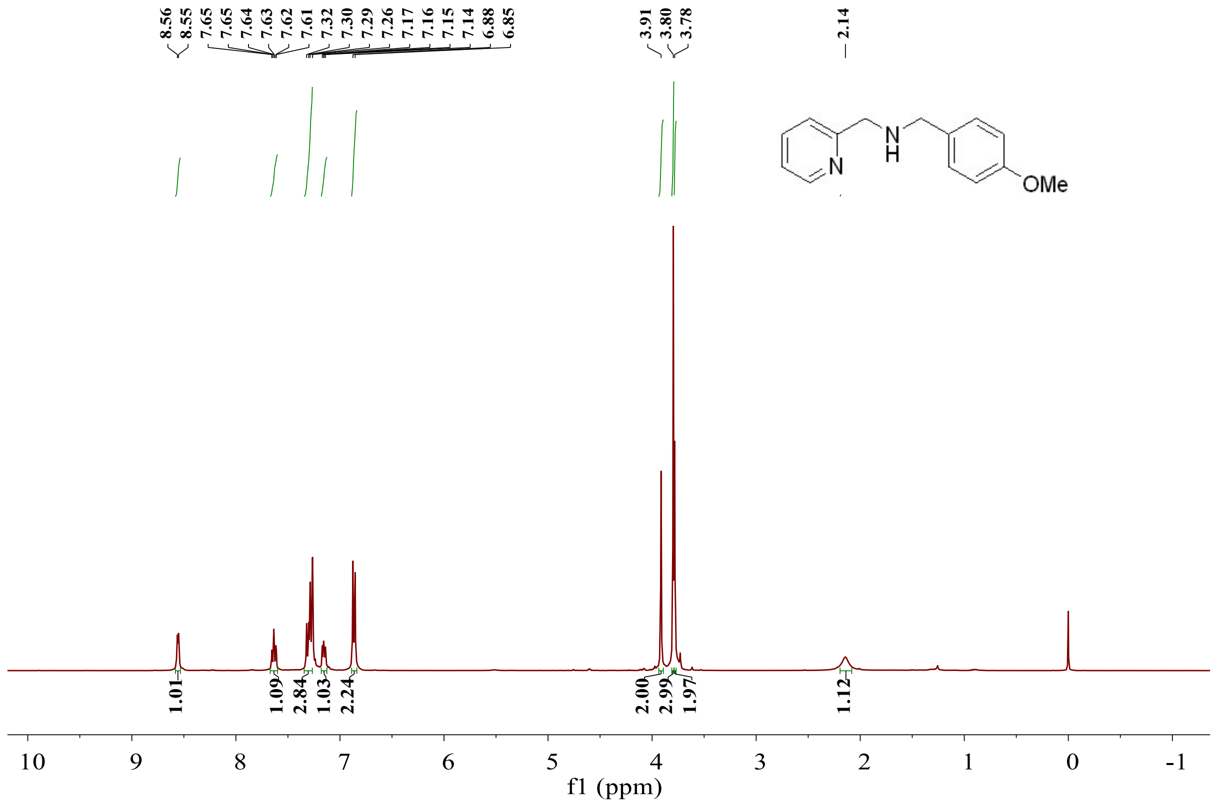

Figure S15. ^{1}H NMR spectrum (400 MHz, $CDCl_3$, 298 K) of $L8_H$

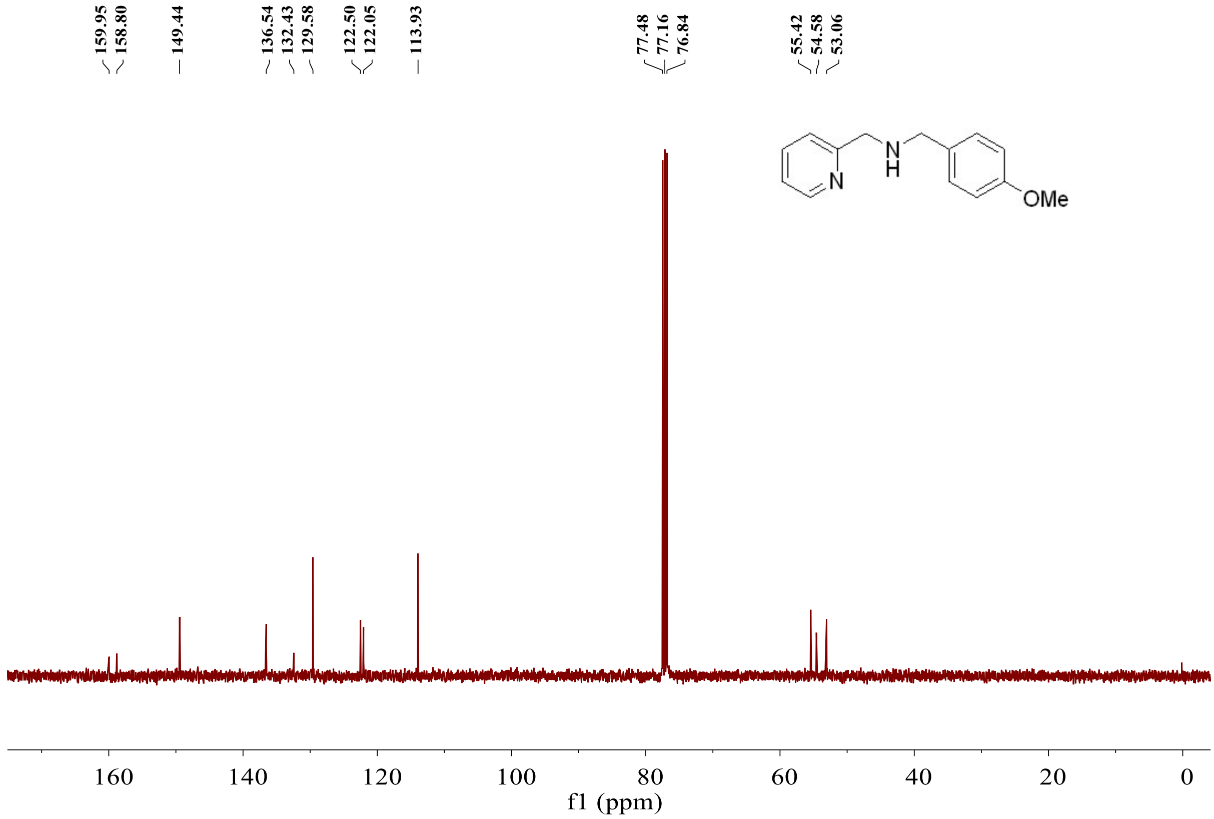

Figure S16. ^{13}C NMR spectrum (100 MHz, $CDCl_3$, 298 K) of $L8_H$

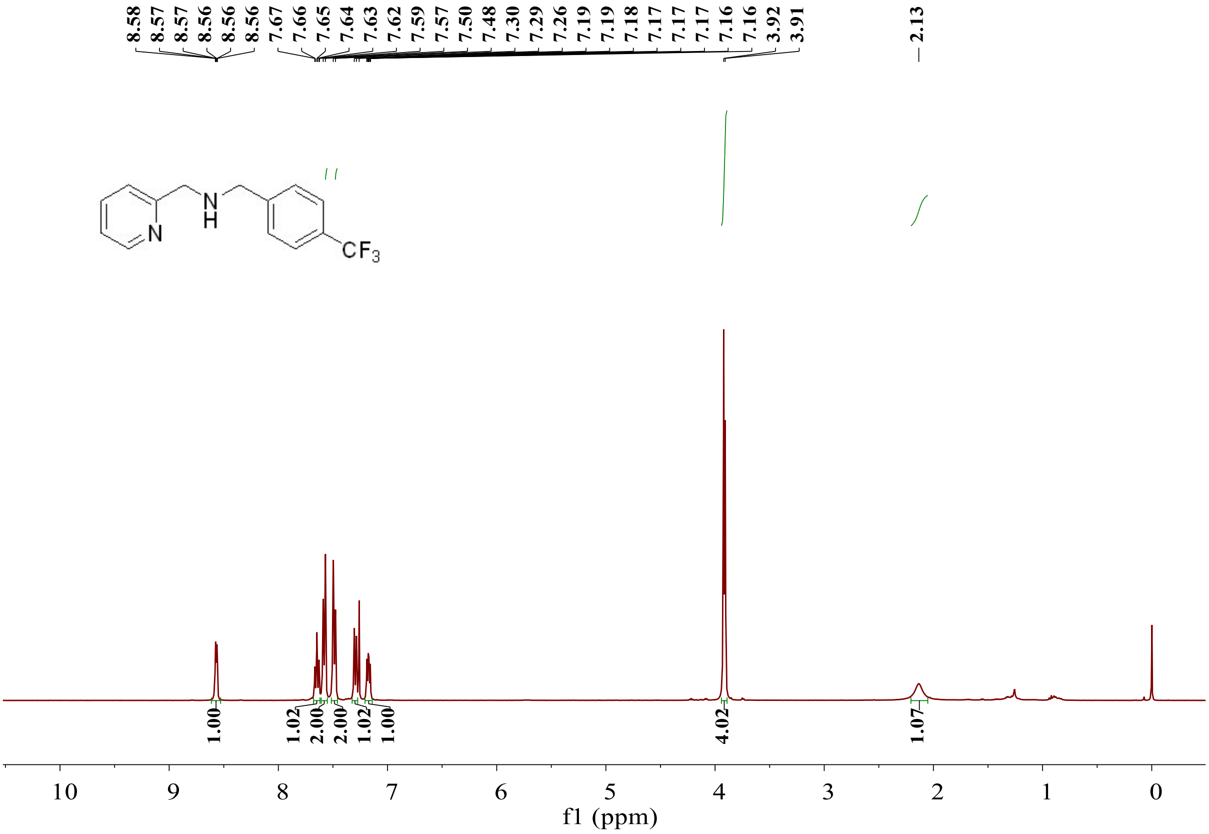

Figure S17. ^{1}H NMR spectrum (400 MHz, $CDCl_3$, 298 K) of $L9_H$

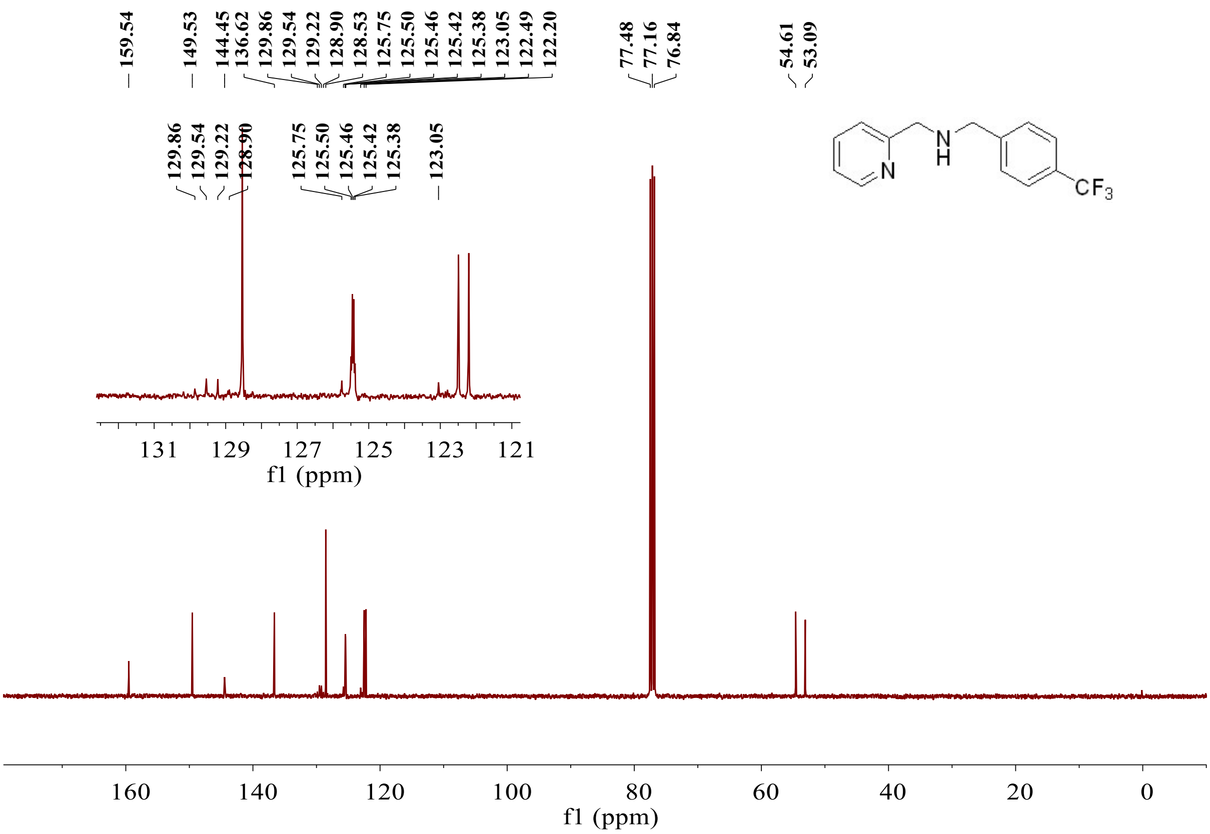

Figure S18. ^{13}C NMR spectrum (100 MHz, $CDCl_3$, 298 K) of $L9_H$

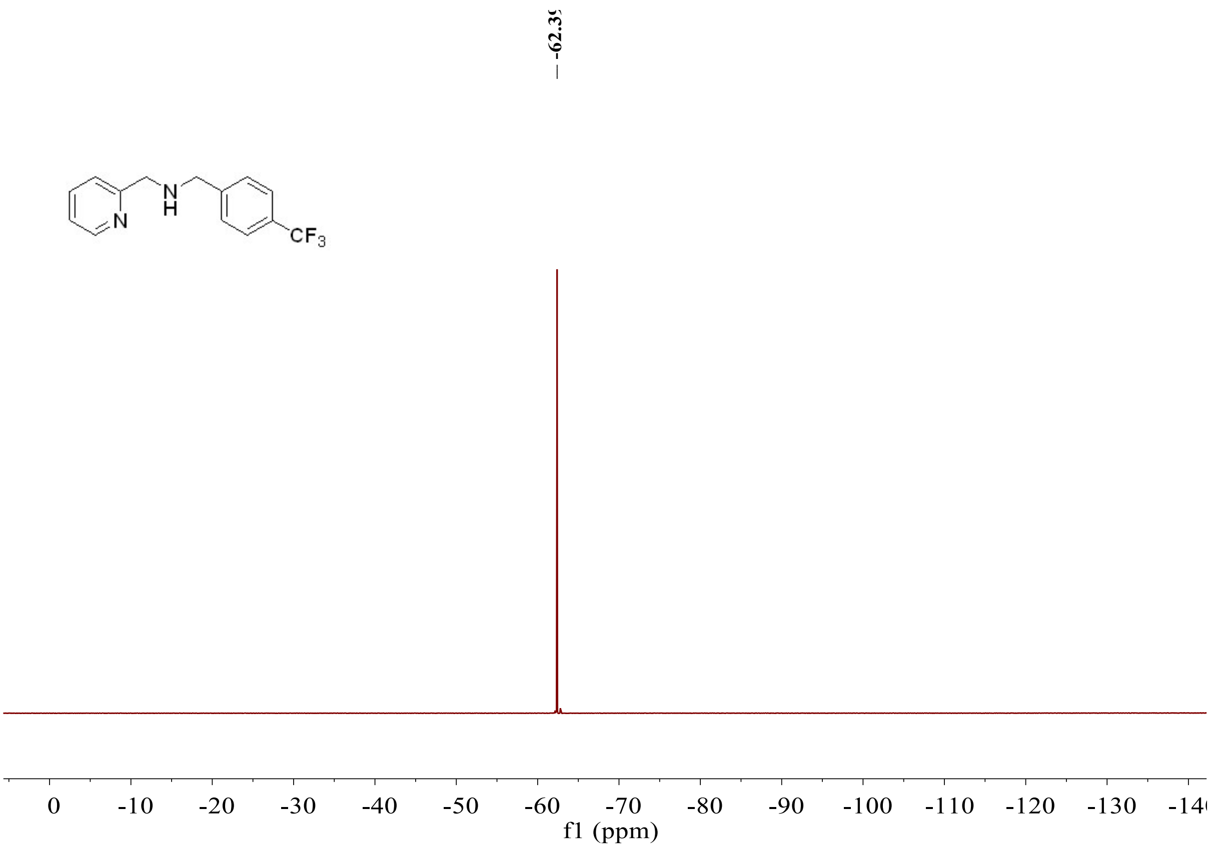

Figure S19. ^{19}F NMR spectrum (376 MHz, $CDCl_3$, 298 K) of $L9_H$

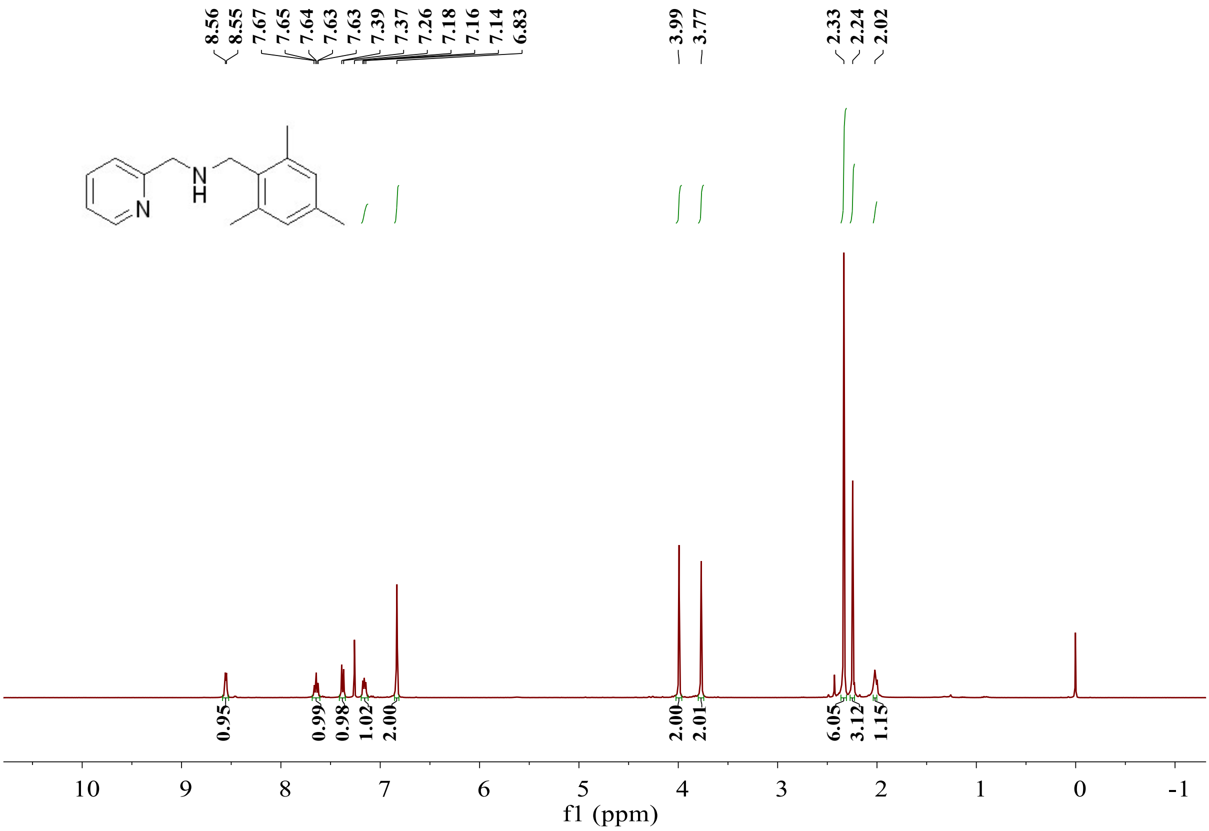

Figure S20. ^{1}H NMR spectrum (400 MHz, $CDCl_3$, 298 K) of $L10_H$

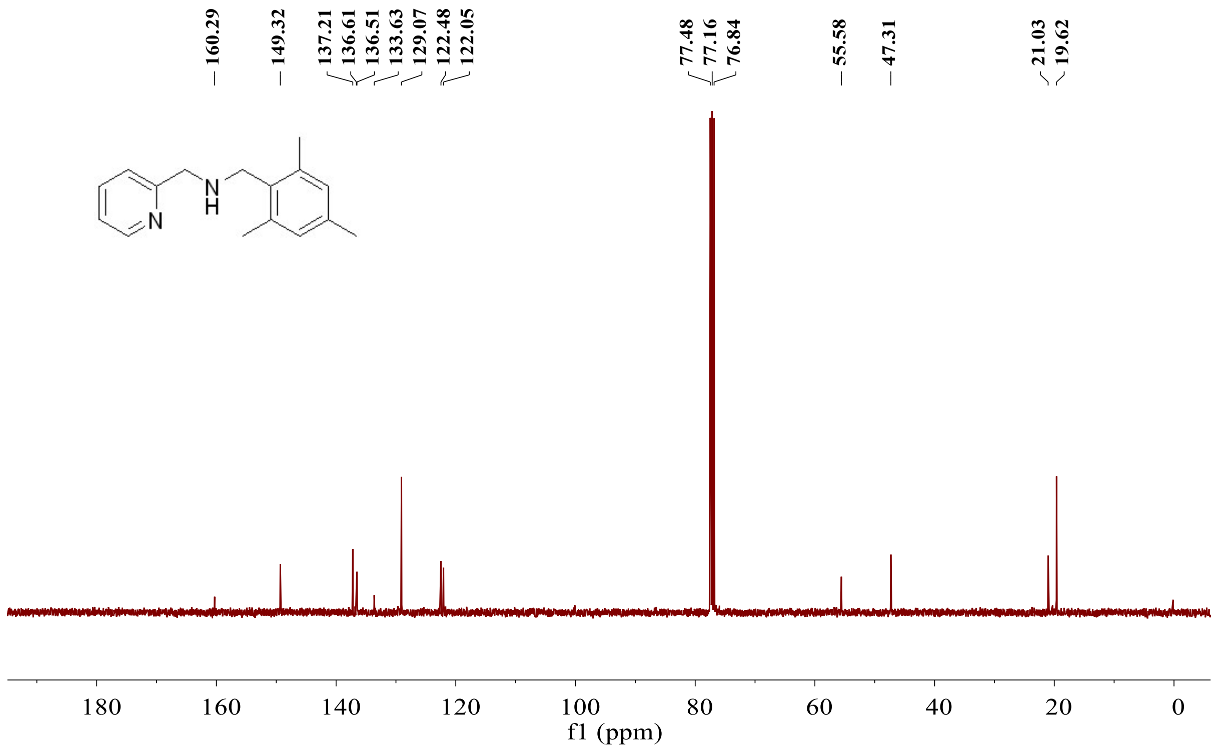

Figure S21. ^{13}C NMR spectrum (100 MHz, $CDCl_3$, 298 K) of $L10_H$

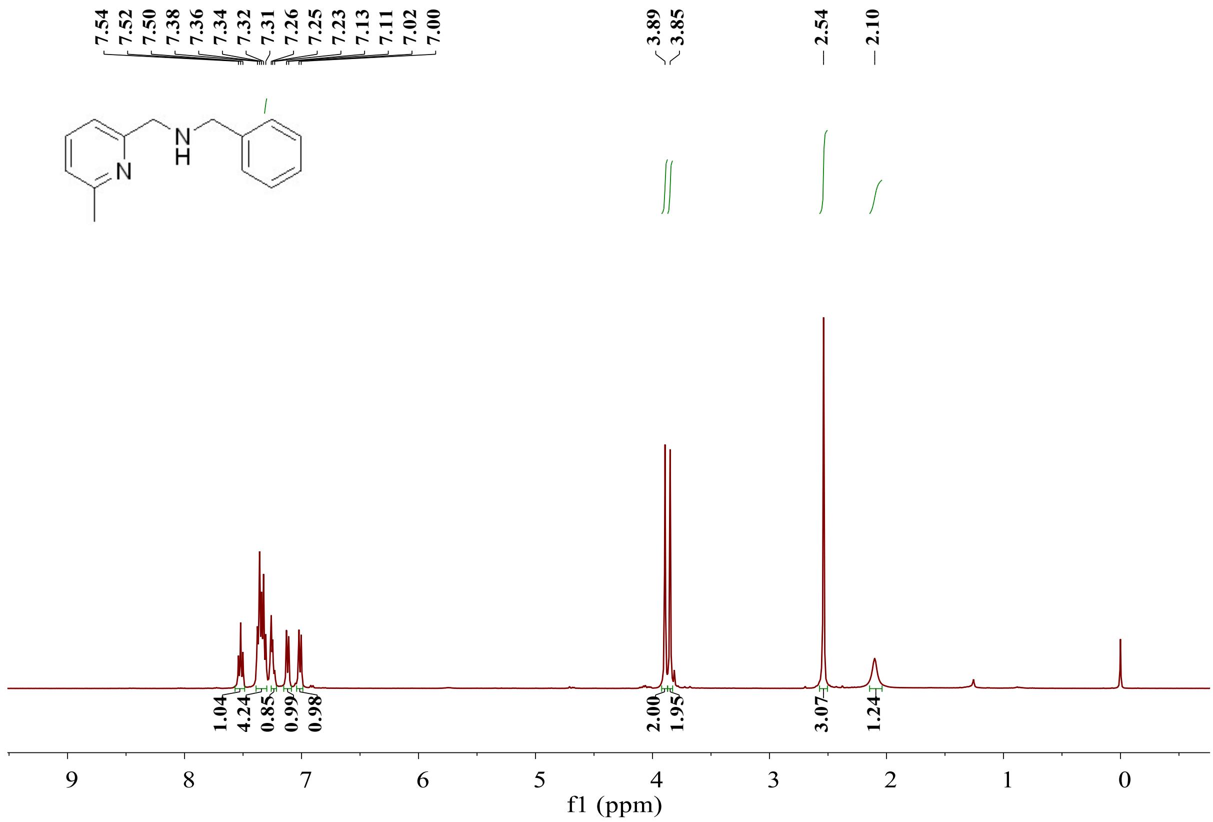

Figure S22. ^1H NMR spectrum (400 MHz, $CDCl_3$, 298 K) of $L11_{Me}$

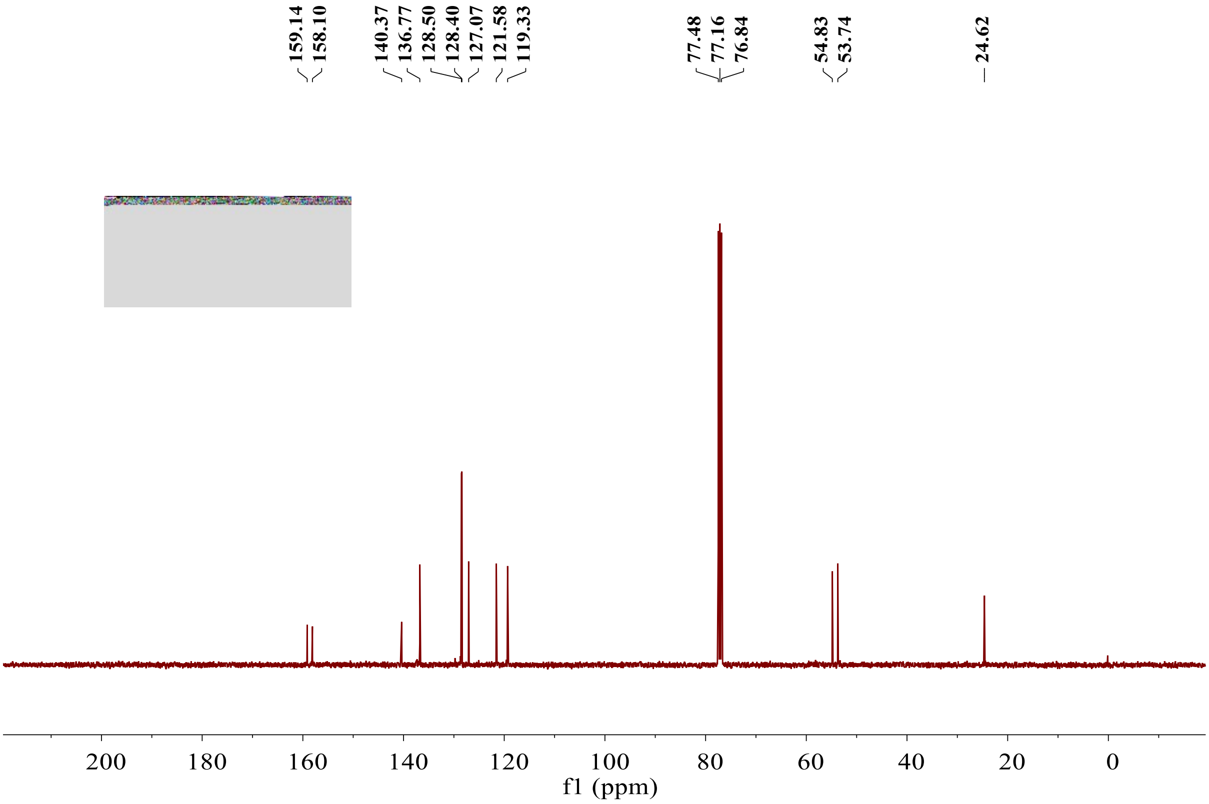

Figure S23. ^{13}C NMR spectrum (100 MHz, $CDCl_3$, 298 K) of $L11_{Me}$

3. NMR Spectra of the Representative Polyisoprene

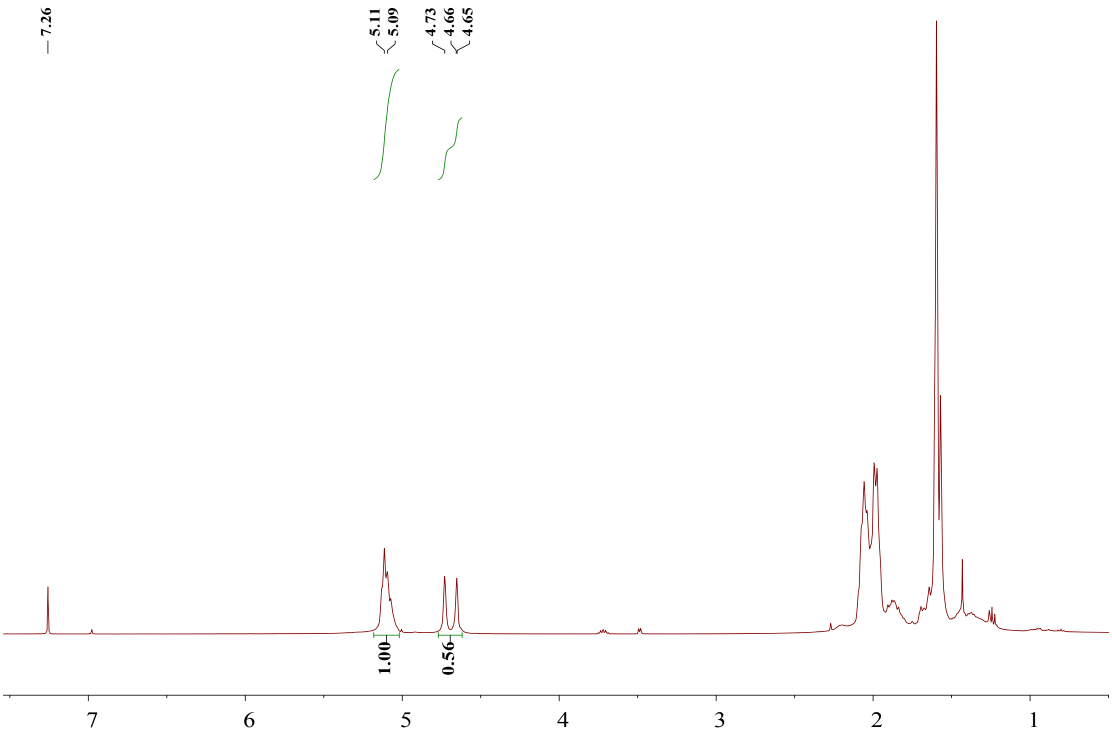

Figure S24. ^{1}H NMR spectrum (400 MHz, $CDCl_3$, 298 K) of polyisoprene (Table 2, entry 2).

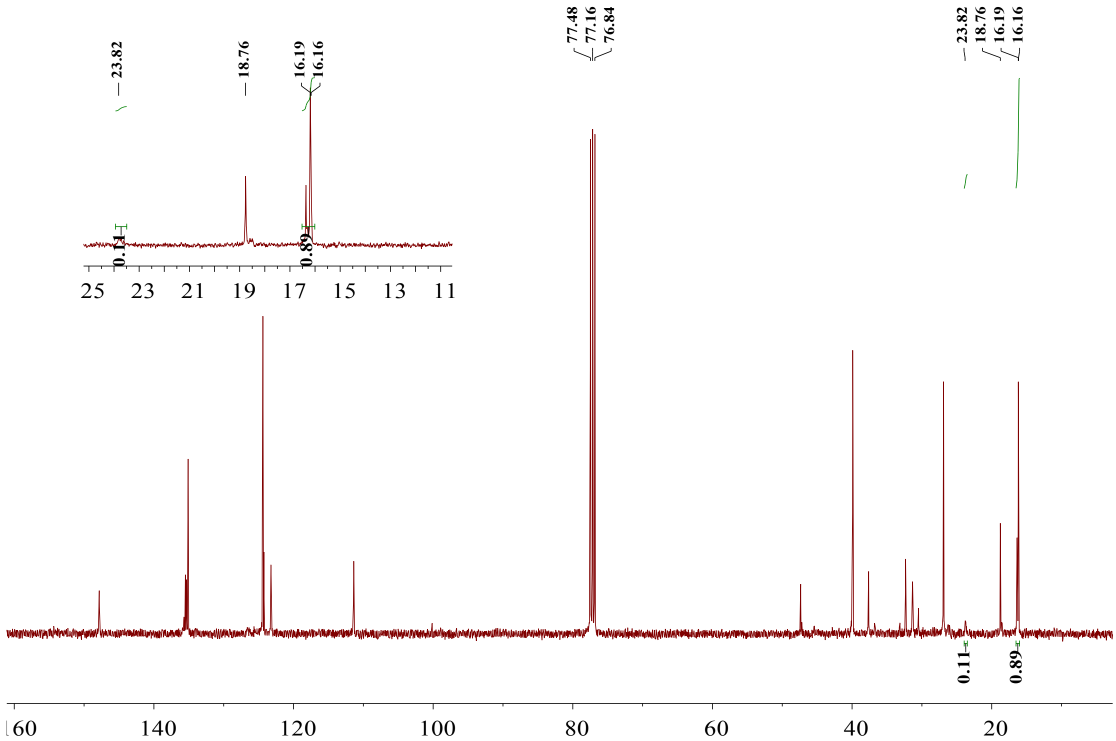

Figure S25. ^{13}C NMR spectrum (100 MHz, $CDCl_3$, 298 K) of polyisoprene (Table 2, entry 2).

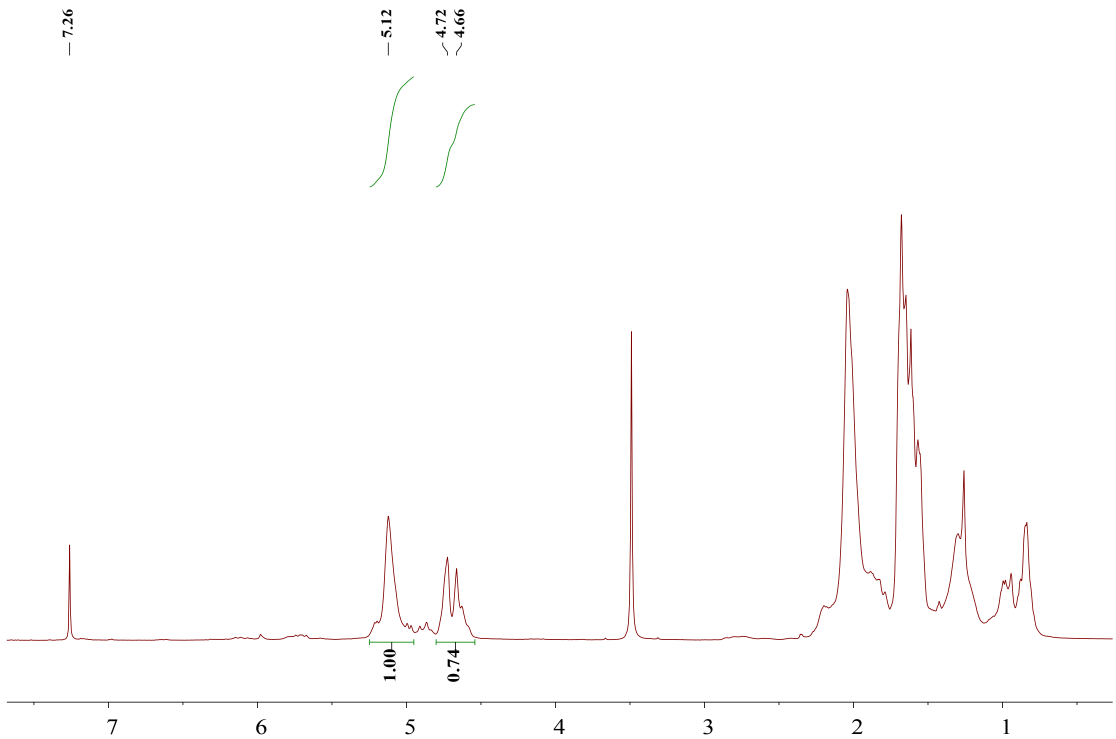

Figure S26. ^{1}H NMR spectrum (400 MHz, $CDCl_3$, 298 K) of polyisoprene (Table 2, entry 3).

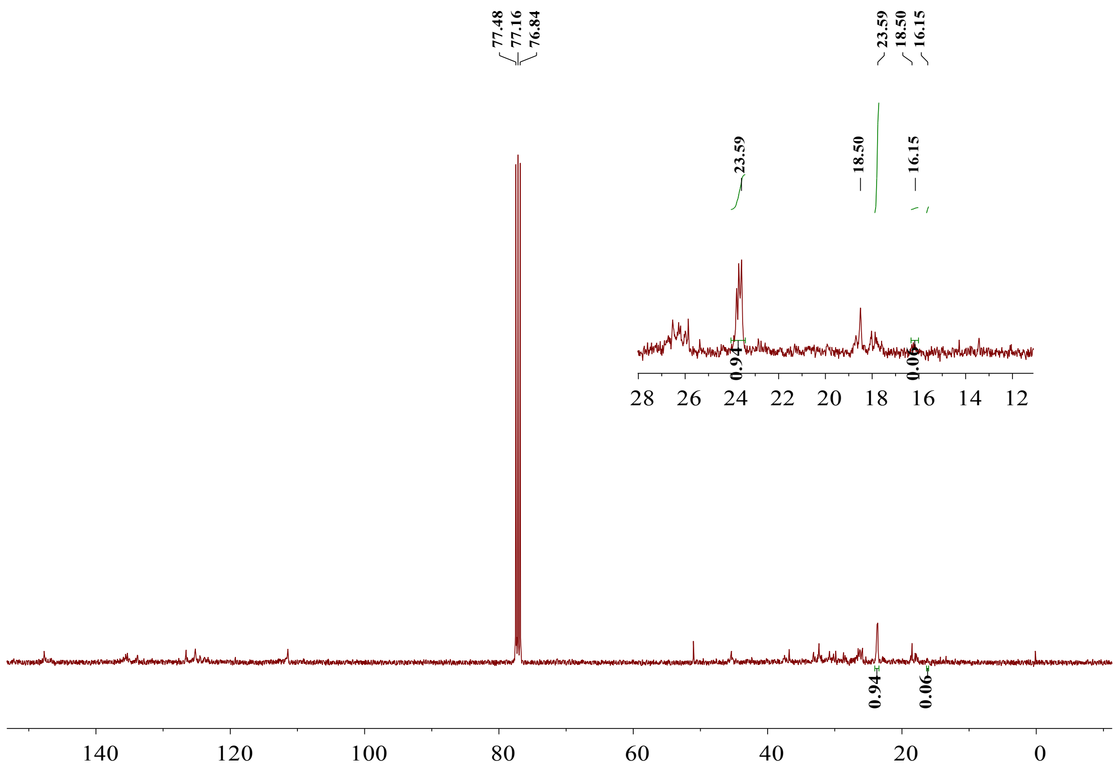

Figure S27. ^{13}C NMR spectrum (100 MHz, $CDCl_3$, 298 K) of polyisoprene (Table 2, entry 3)

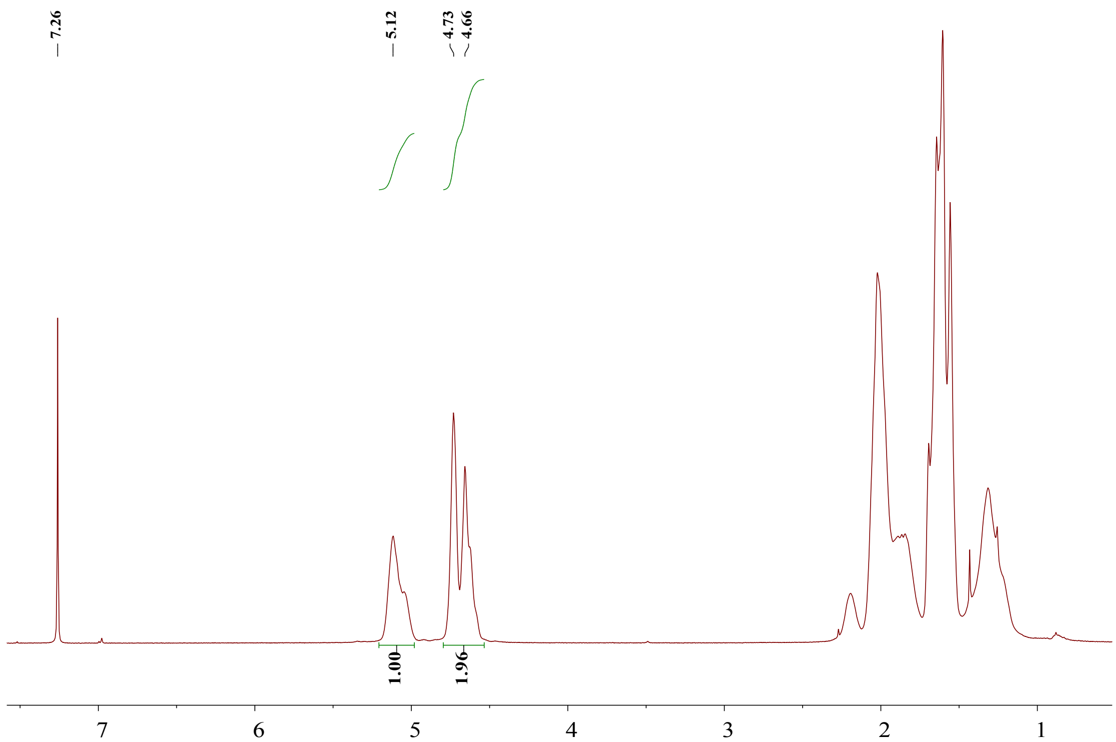

Figure S28. ^{1}H NMR spectrum (400 MHz, $CDCl_3$, 298 K) of polyisoprene (Table 2, entry 6).

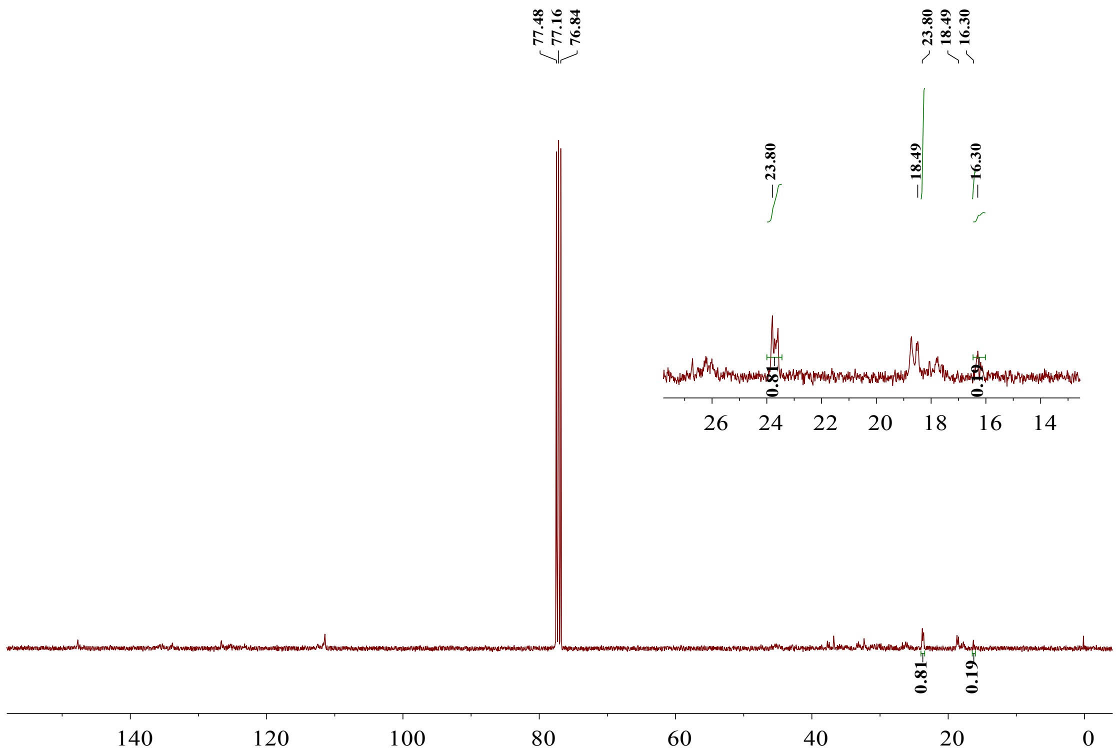

Figure S29. ^{13}C NMR spectrum (100 MHz, $CDCl_3$, 298 K) of polyisoprene (Table 2, entry 6)

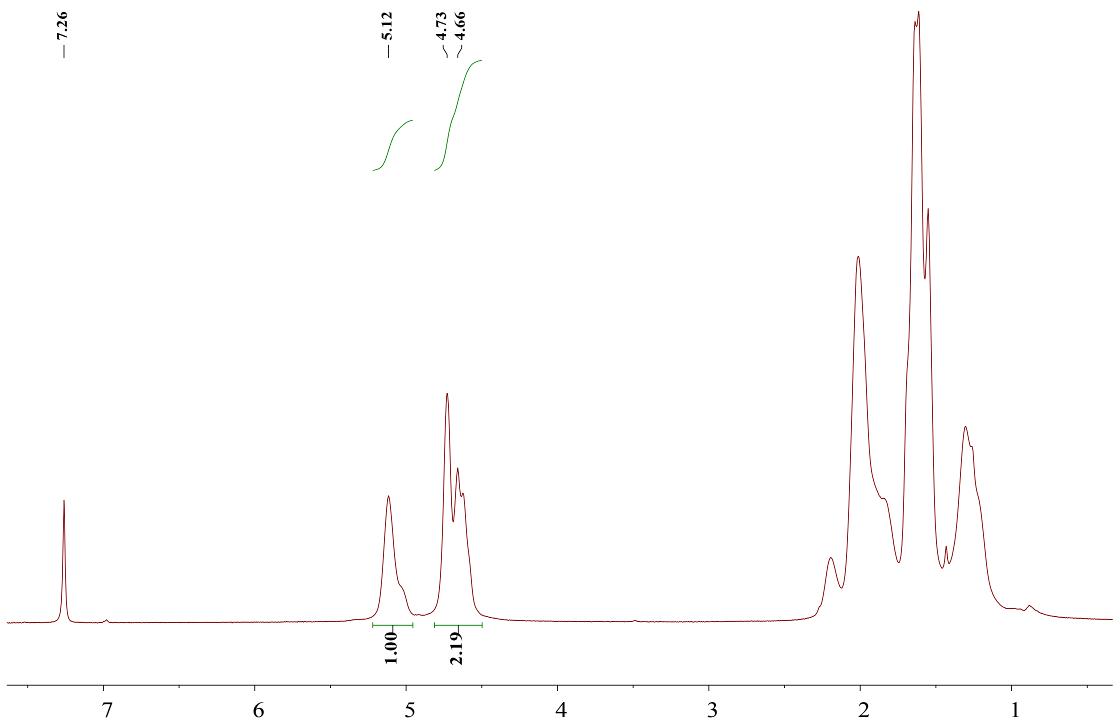

Figure S30. ^{1}H NMR spectrum (400 MHz, $CDCl_3$, 298 K) of polyisoprene (Table 2, entry 7).

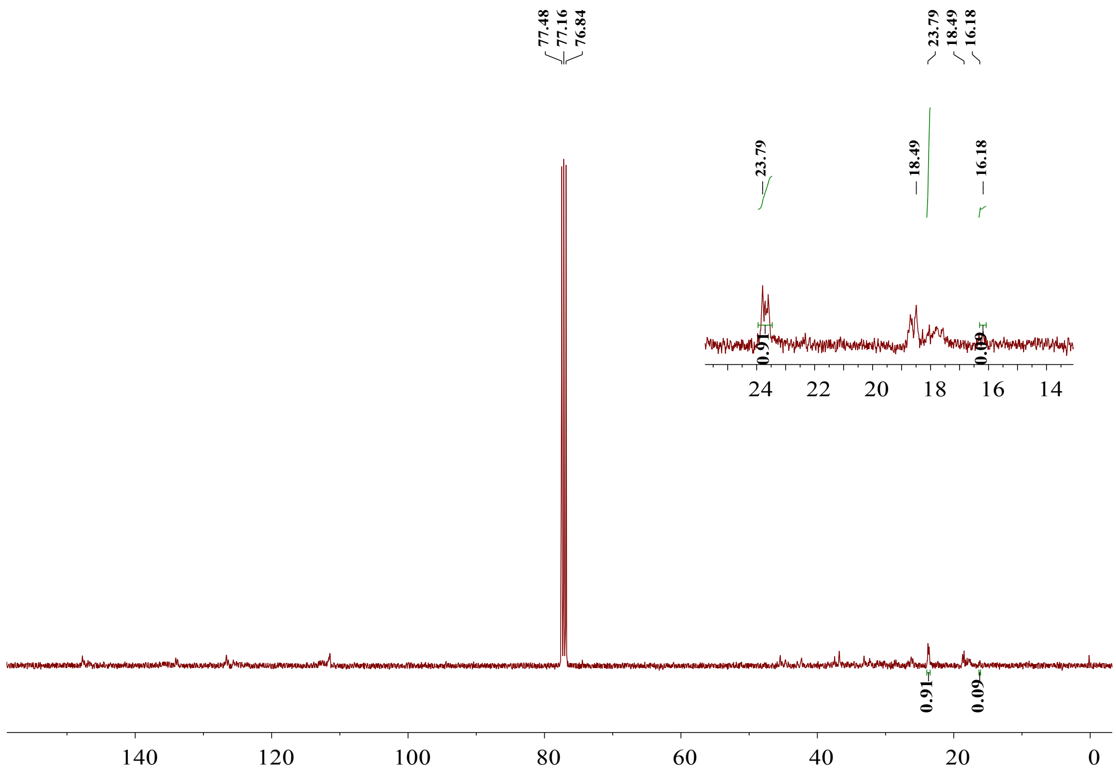

Figure S31. ^{13}C NMR spectrum (100 MHz, $CDCl_3$, 298 K) of polyisoprene (Table 2, entry 7)

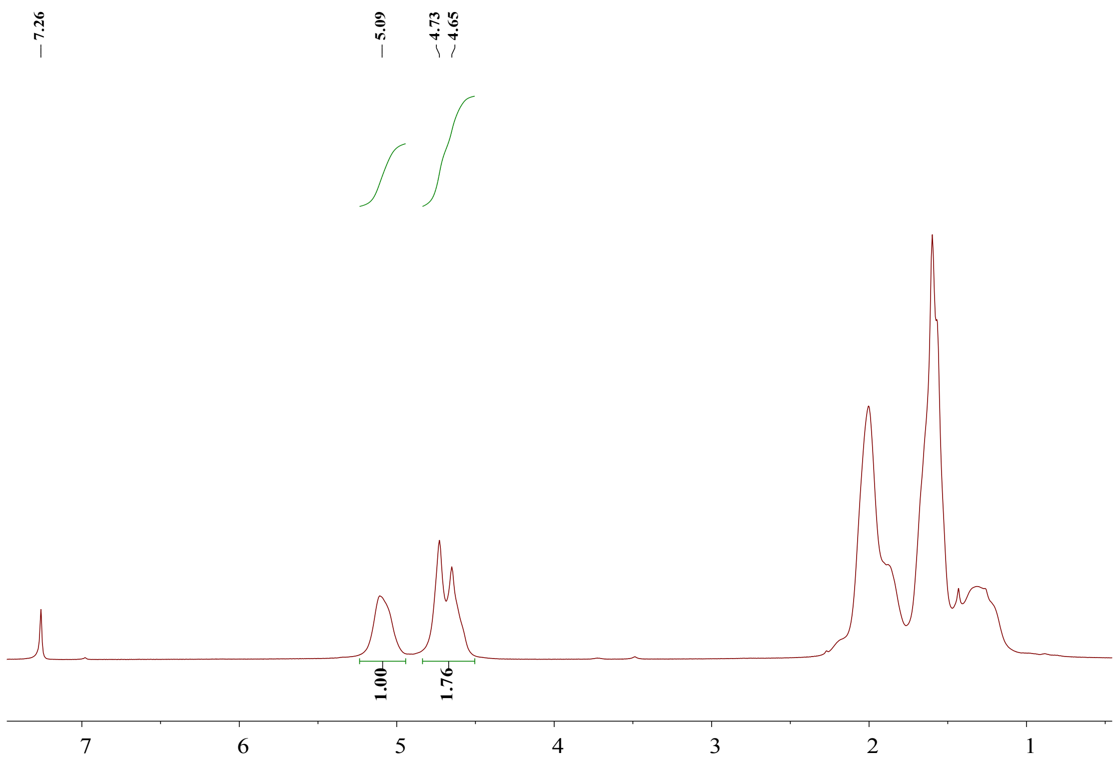

Figure S32. ^{1}H NMR spectrum (400 MHz, $CDCl_3$, 298 K) of polyisoprene (Table 3, entry 3)

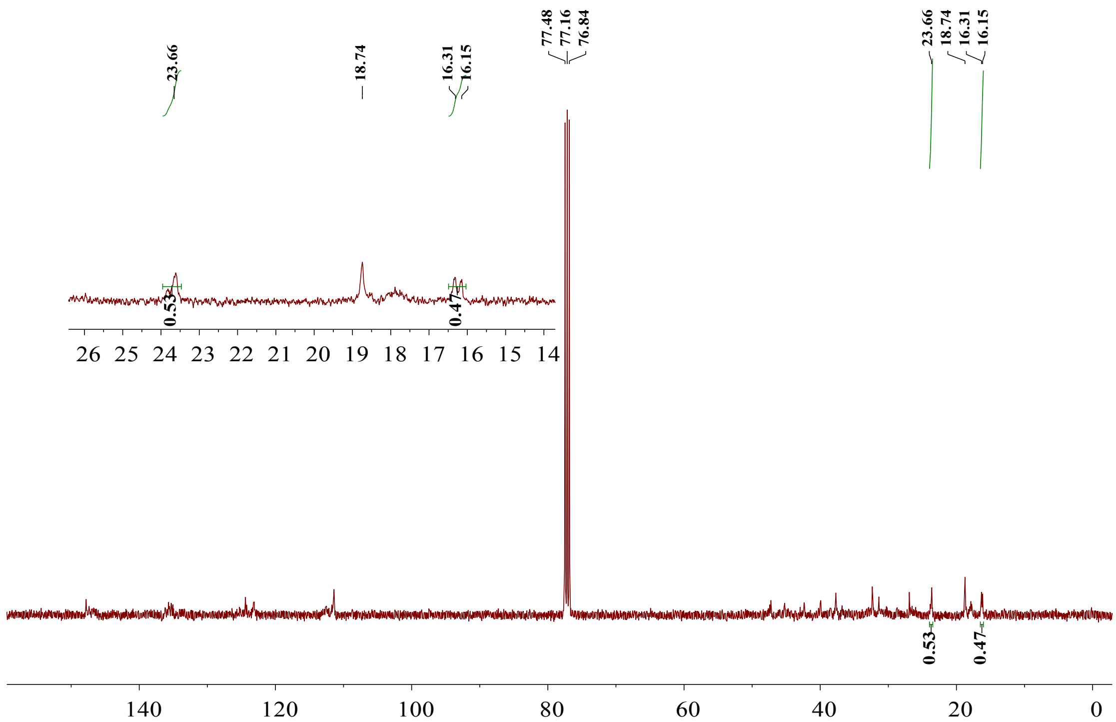

Figure S33. ^{13}C NMR spectrum (100 MHz, $CDCl_3$, 298 K) of polyisoprene (Table 3, entry 3)

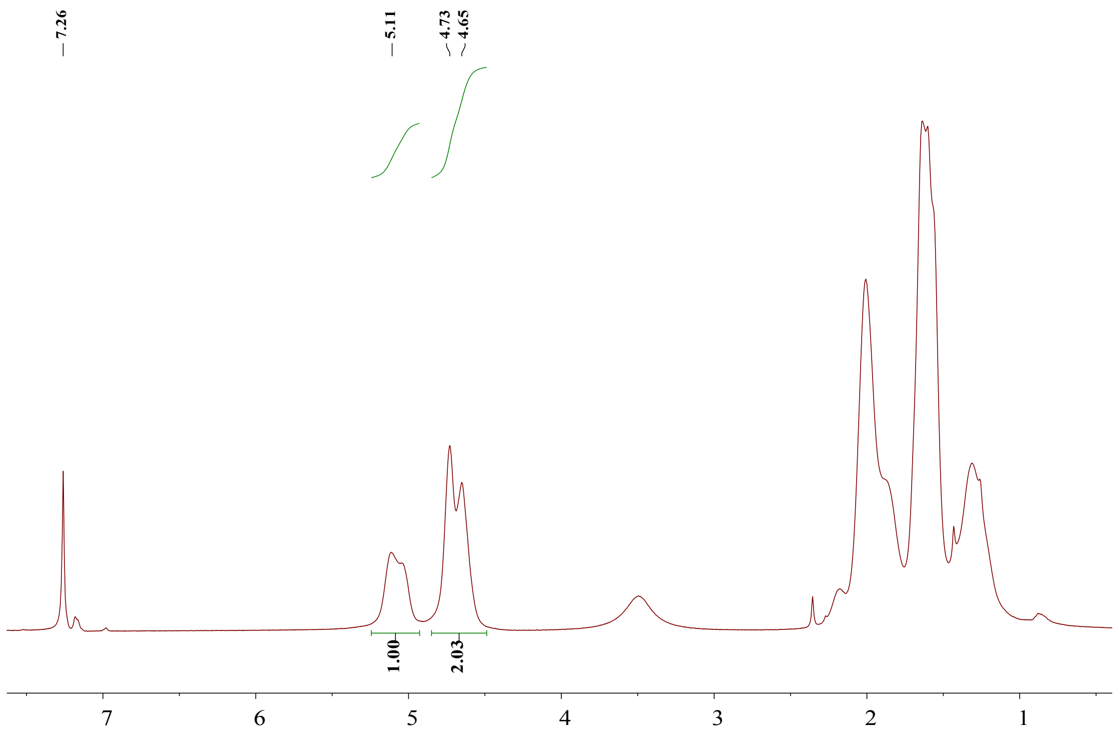

Figure S34. ^{1}H NMR spectrum (400 MHz, $CDCl_3$, 298 K) of polyisoprene (Table 3, entry 6)

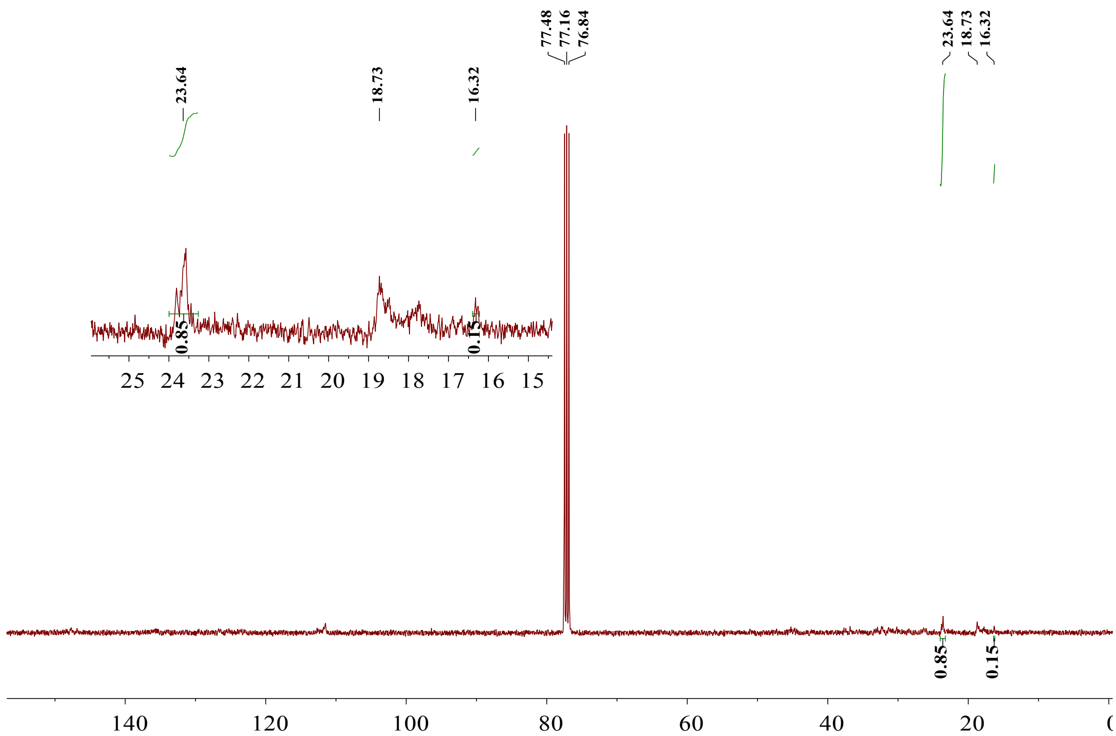

Figure S35. ^{13}C NMR spectrum (100 MHz, $CDCl_3$, 298 K) of polyisoprene (Table 3, entry 6)

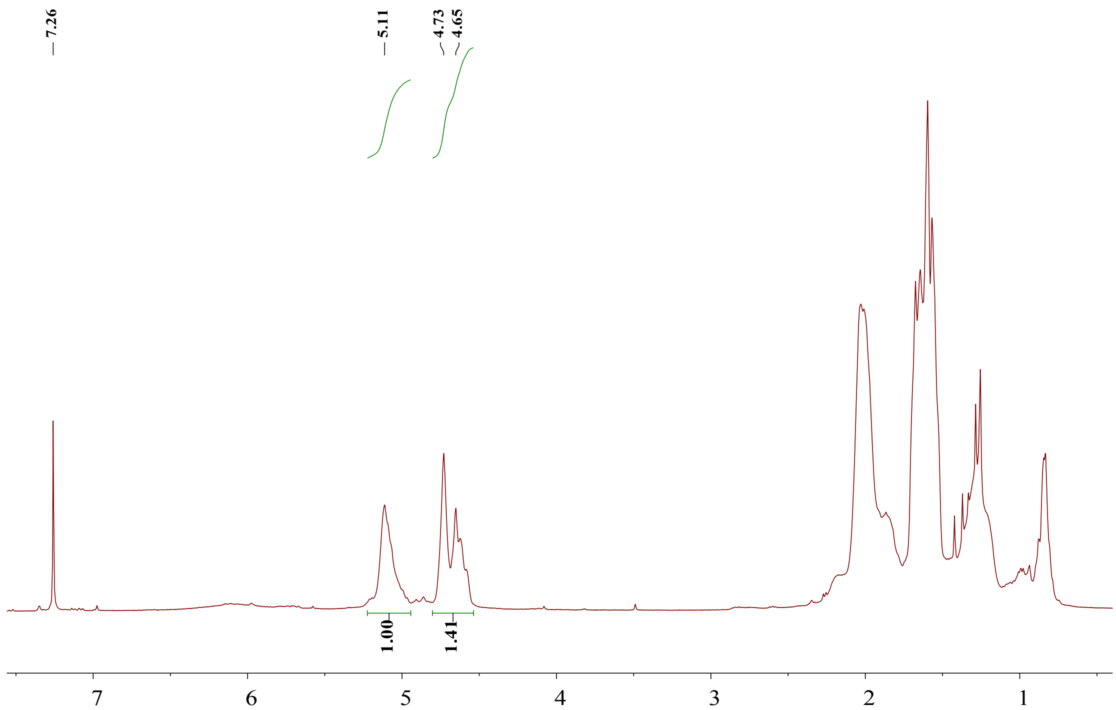

Figure S36. ^{1}H NMR spectrum (400 MHz, $CDCl_3$, 298 K) of polyisoprene (Table 3, entry 11)

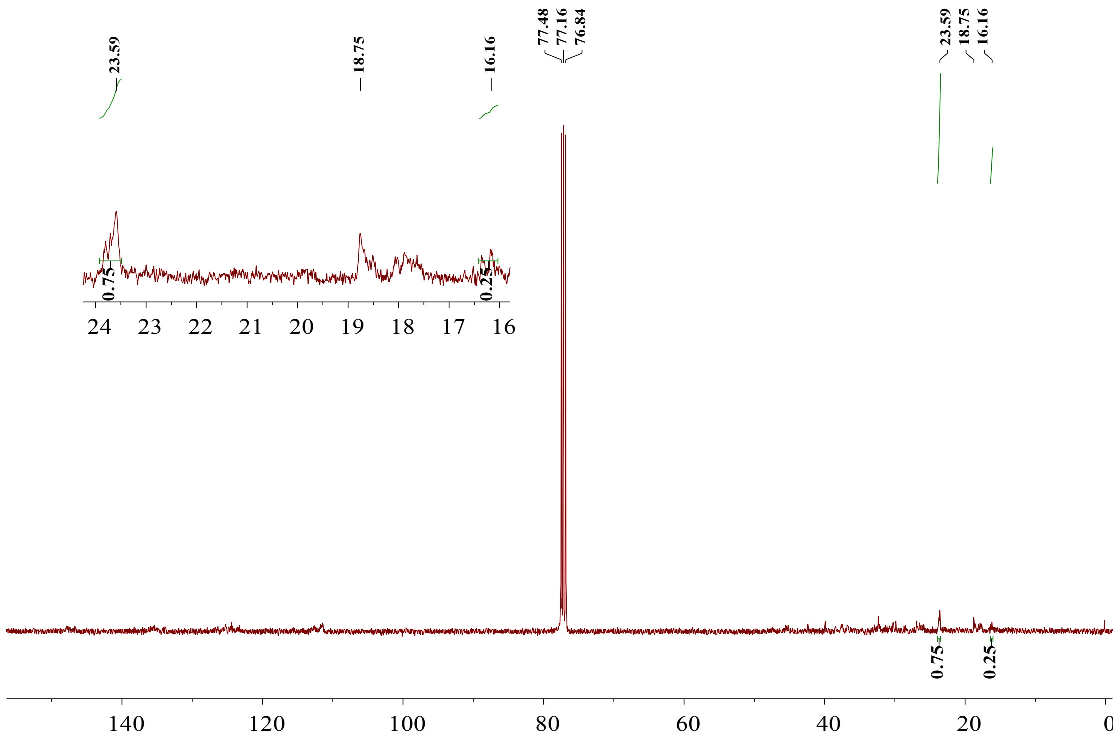

Figure S37. ^{13}C NMR spectrum (100 MHz, $CDCl_3$, 298 K) of polyisoprene (Table 3, entry 11)

4. GPC Characterization of the Representative Polyisoprene

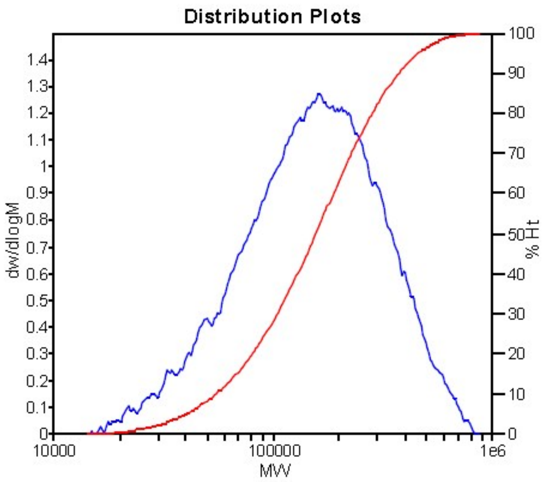

Figure S38. the GPC of Fe(II) complex **Fe1$_H$** catalyzed polyisoprene (Table 2, entry 1).

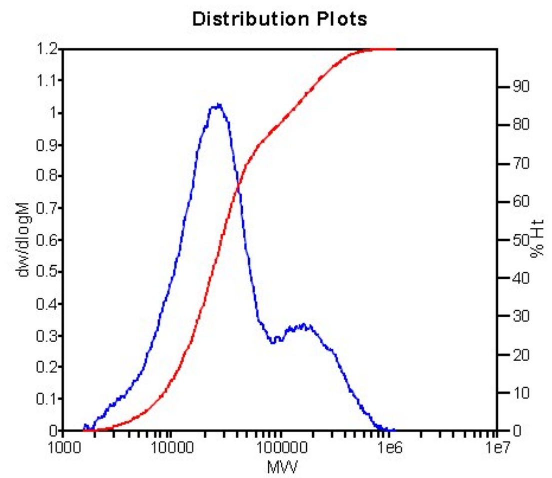

Figure S39. the GPC of Fe(II) complex **Fe2$_H$** catalyzed polyisoprene (Table 2, entry 2)

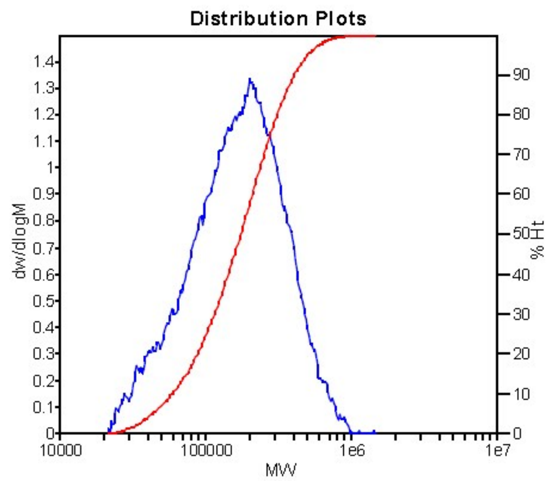

Figure S40. the GPC of Fe(II) complex **Fe3$_{Me}$** catalyzed polyisoprene (Table 2, entry 3)

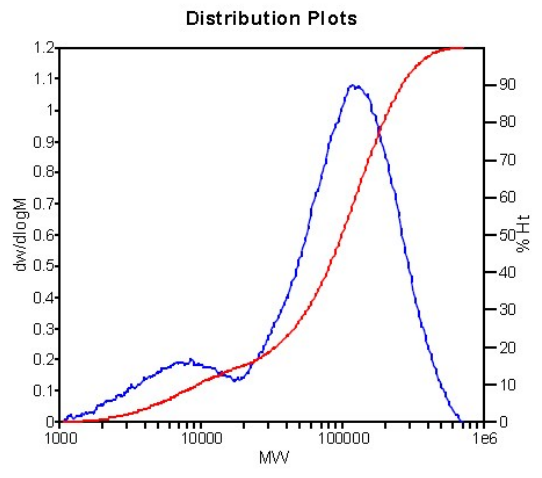

Figure S41. the GPC of Fe(II) complex **Fe4$_H$** catalyzed polyisoprene (Table 2, entry 4)

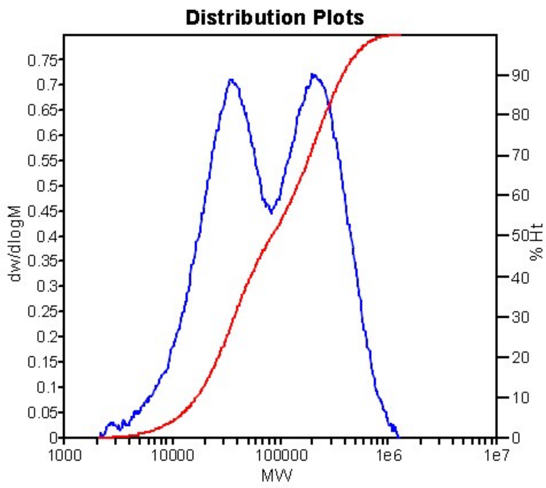

Figure S42. the GPC of Fe(II) complex **$Fe5_H$** catalyzed polyisoprene (Table 2, entry 5)

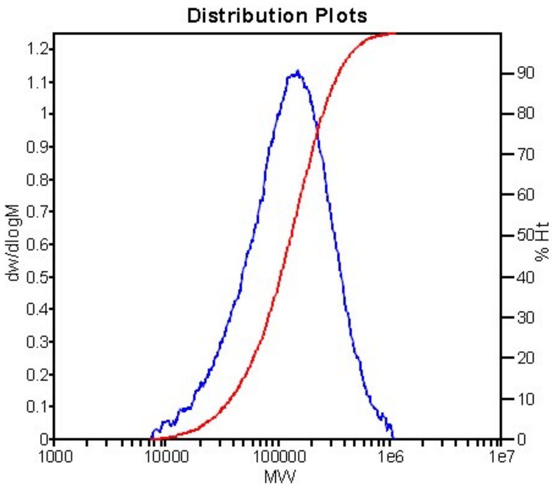

Figure S43. the GPC of Fe(II) complex **$Fe6_H$** catalyzed polyisoprene (Table 2, entry 6)

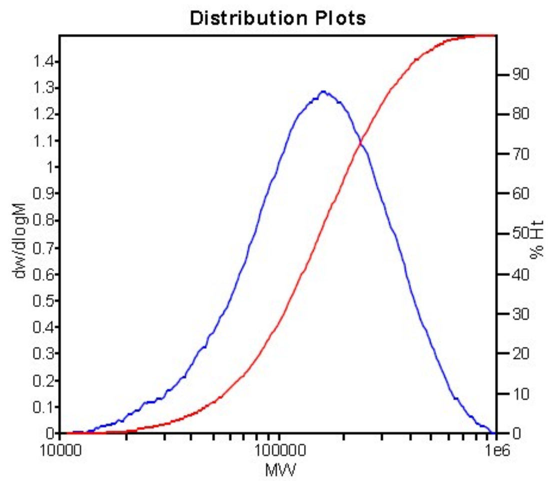

Figure S44. the GPC of Fe(II) complex **$Fe7_H$** catalyzed polyisoprene (Table 2, entry 7)

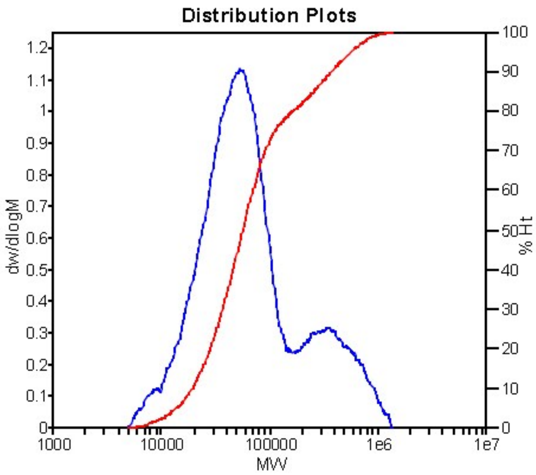

Figure S45. the GPC of Fe(II) complex **Fe8$_H$** catalyzed polyisoprene (Table 3, entry 8)

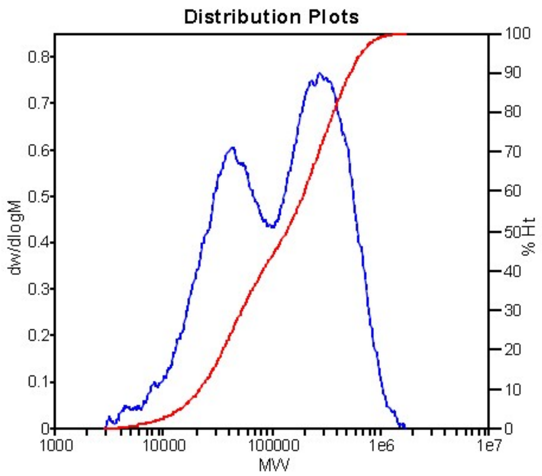

Figure S46. the GPC of Fe(II) complex **Fe9$_H$** catalyzed polyisoprene (Table 3, entry 9)

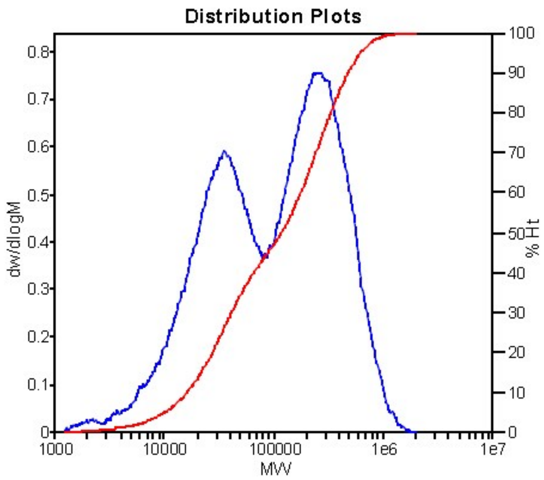

Figure S47. the GPC of Fe(II) complex **Fe10$_H$** catalyzed polyisoprene (Table 3, entry 10)

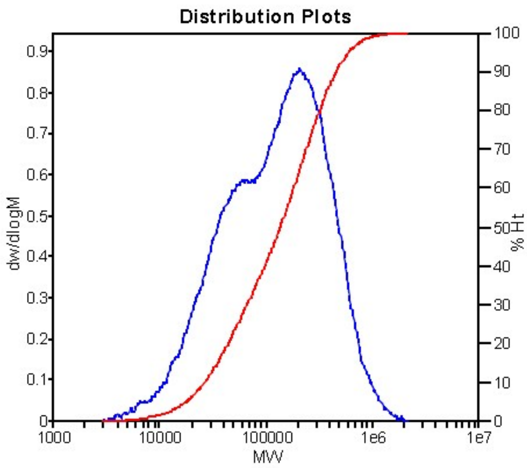

Figure S48. the GPC of Fe(II) complex **$Fe11_{Me}$** catalyzed polyisoprene (Table 3, entry 11)

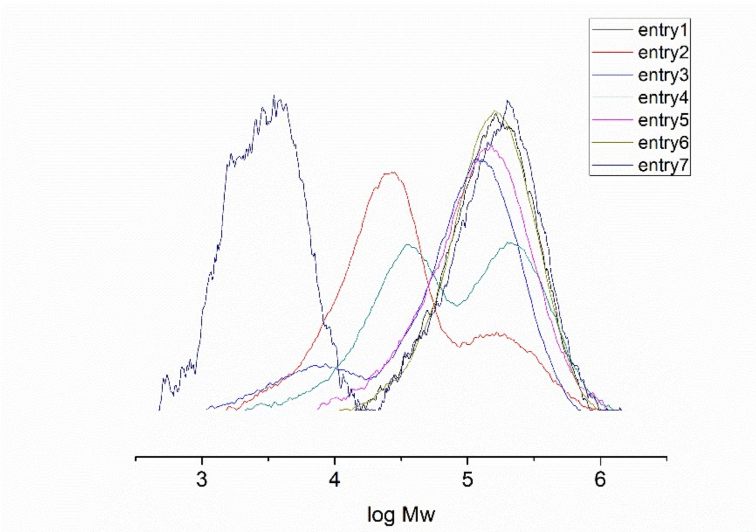

Figure S49 the GPC of Fe(II) complex **$Fe1_H$ – $Fe7_H$** catalyzed polyisoprene (Table 2, entries 1 – 7)

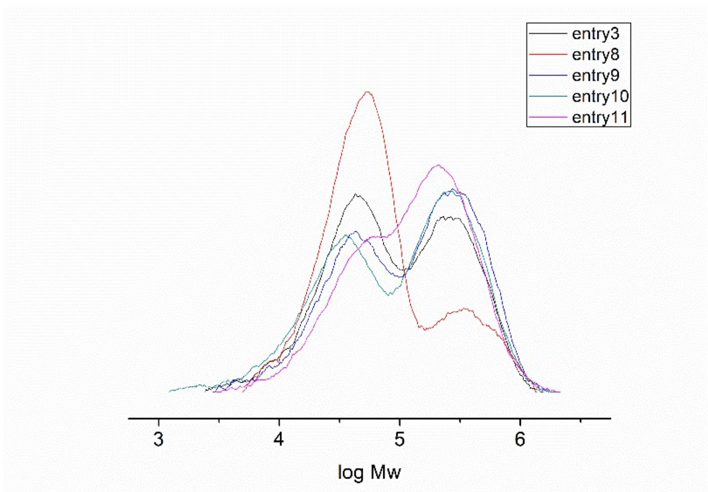

Figure S50 the GPC of Fe(II) complex **$Fe5_H$, $Fe8_H$ – $Fe11_{Me}$** catalyzed polyisoprene (Table 3, entries 3, 8 – 11)

5. X-Ray Crystallography of Complexes

Fe3$_{Me}$:CCDC number: 1884670**;**

Abstract

Table 1

Experimental details

Crystal data	
Chemical formula	$C_{20}H_{20}Cl_2FeN_2$
M_r	415.13
Crystal system, space group	Triclinic, $P\overline{1}$
Temperature (K)	298
a, *b*, *c* (Å)	8.9981 (8), 10.7524 (9), 11.3021 (11)
α, β, γ (°)	89.495 (3), 66.730 (1), 79.902 (2)
V (Å^3)	986.77 (15)
Z	2
Radiation type	Mo *K*α
μ (mm^{-1})	1.04
Crystal size (mm)	0.22 × 0.15 × 0.10
Data collection	
Diffractometer	CCD area detector
Absorption correction	Multi-scan *SADABS*
T_{min}, T_{max}	0.804, 0.903
No. of measured, independent and observed [$I > 2\sigma(I)$] reflections	5011, 3435, 2225
R_{int}	0.048
$(\sin \theta/\lambda)_{max}$ (Å^{-1})	0.595
Refinement	
$R[F^2 > 2\sigma(F^2)]$, $wR(F^2)$, *S*	0.054, 0.126, 1.01
No. of reflections	3435
No. of parameters	227
No. of restraints	12
H-atom treatment	H-atom parameters constrained
$\Delta\rho_{max}$, $\Delta\rho_{min}$ (e Å^{-3})	0.49, −0.56

Computer programs: Bruker *SMART*, Bruker *SHELXTL*, *SHELXS97* (Sheldrick, 1990), *SHELXL2018*/3 (Sheldrick, 2018).

References

NOT FOUND

Fe7$_H$:1884491

Abstract

Table 1

Experimental details

Crystal data	
Chemical formula	$C_{12}H_{18}Cl_2FeN_2$
M_r	317.03
Crystal system, space group	Orthorhombic, *Pbca*
Temperature (K)	293
a, *b*, *c* (Å)	9.1540 (8), 6.8673 (6), 42.281 (3)
V (Å^3)	2657.9 (4)
Z	8
Radiation type	Cu *Kα*
μ (mm^{-1})	12.62
Crystal size (mm)	0.30 × 0.15 × 0.05
Data collection	
Diffractometer	Xcalibur, Eos, Gemini
Absorption correction	Multi-scan *SADABS*
T_{min}, T_{max}	0.116, 0.571
No. of measured, independent and observed [$I > 2\sigma(I)$] reflections	13972, 2242, 1618
R_{int}	0.115
$(\sin \theta/\lambda)_{max}$ (Å^{-1})	0.593
Refinement	
$R[F^2 > 2\sigma(F^2)]$, $wR(F^2)$, S	0.099, 0.223, 1.09
No. of reflections	2242
No. of parameters	154
H-atom treatment	H-atom parameters constrained $w = 1/[\sigma^2(F_o^2) + (0.0583P)^2 + 28.0462P]$ where $P = (F_o^2 + 2F_c^2)/3$
$\Delta\rho_{max}$, $\Delta\rho_{min}$ (e Å^{-3})	1.61, −0.73

Computer programs: *SHELXL2018*/3 (Sheldrick, 2018).

Table 2

Hydrogen-bond geometry (Å, °) for (1884491)

D—H···*A*	*D*—H	H···*A*	*D*···*A*	*D*—H···*A*
C8—H8*A*···Cl2^{i}	0.97	2.83	3.538 (10)	131
C7—H7···Cl2	0.98	2.85	3.451 (10)	121
C6—H6···Cl1	0.93	2.95	3.525 (10)	121
C8—H8*A*···Cl2^{i}	0.97	2.83	3.538 (10)	131
C7—H7···Cl2	0.98	2.85	3.451 (10)	121
C6—H6···Cl1	0.93	2.95	3.525 (10)	121
C8—H8*A*···Cl2^{i}	0.97	2.83	3.538 (10)	131

C7—H7···Cl2	0.98	2.85	3.451 (10)	121
C6—H6···Cl1	0.93	2.95	3.525 (10)	121
C8—H8*A*···Cl2^{i}	0.97	2.83	3.538 (10)	131
C7—H7···Cl2	0.98	2.85	3.451 (10)	121
C6—H6···Cl1	0.93	2.95	3.525 (10)	121
C6—H6···Cl1	0.93	2.95	3.525 (10)	121
C7—H7···Cl2	0.98	2.85	3.451 (10)	121
C8—H8*A*···Cl2^{i}	0.97	2.83	3.538 (10)	131
C6—H6···Cl1	0.93	2.95	3.525 (10)	121
C7—H7···Cl2	0.98	2.85	3.451 (10)	121
C8—H8*A*···Cl2^{i}	0.97	2.83	3.538 (10)	131
C6—H6···Cl1	0.93	2.95	3.525 (10)	121
C7—H7···Cl2	0.98	2.85	3.451 (10)	121
C8—H8*A*···Cl2^{i}	0.97	2.83	3.538 (10)	131

Symmetry code: (i) $-x+1/2, y+1/2, z$.

References

NOT FOUND

$Fe4_H$: 1884672;

Abstract

Table 1

Experimental details

Crystal data	
Chemical formula	$C_{28}H_{32}Cl_4Fe_2N_4$
M_r	678.07
Crystal system, space group	Monoclinic, *C*2/*c*
Temperature (K)	298
a, *b*, *c* (Å)	15.1785 (13), 9.3366 (8), 22.6274 (18)
β (°)	103.782 (2)
V (Å³)	3114.3 (5)
Z	4
Radiation type	Mo *K*α
μ (mm^{-1})	1.30
Crystal size (mm)	0.16 × 0.11 × 0.10
Data collection	
Diffractometer	CCD area detector
Absorption correction	Multi-scan *SADABS*
T_{min}, T_{max}	0.819, 0.881
No. of measured, independent and observed [$I > 2\sigma(I)$] reflections	7713, 2739, 1864
R_{int}	0.038
$(\sin \theta/\lambda)_{max}$ (Å^{-1})	0.595
Refinement	
$R[F^2 > 2\sigma(F^2)]$, $wR(F^2)$, S	0.034, 0.072, 1.04
No. of reflections	2739
No. of parameters	189
No. of restraints	24
H-atom treatment	H-atom parameters constrained
$\Delta\rho_{max}$, $\Delta\rho_{min}$ (e Å^{-3})	0.34, −0.22

Computer programs: *SHELXL2018*/3 (Sheldrick, 2018).

Table 2

Hydrogen-bond geometry (Å, º) for (1884672)

D—H···*A*	*D*—H	H···*A*	*D*···*A*	*D*—H···*A*
C5—H5···Cl2^{i}	0.93	2.95	3.867 (3)	168
C6—H6···Cl1^{ii}	0.93	2.83	3.431 (3)	123
C8—H8···Cl1	0.98	2.96	3.488 (3)	115

Symmetry codes: (i) −*x*+1, −*y*+1, −*z*+2; (ii) −*x*+1, −*y*+2, −*z*+2.

Fe11$_{Me}$: 1884671

Abstract

Table 1

Experimental details

Crystal data	
Chemical formula	$C_{14}H_{16}Cl_2FeN_2$
M_r	339.04
Crystal system, space group	Monoclinic, $P2_1/c$
Temperature (K)	298
a, b, c (Å)	7.0439 (7), 13.0684 (11), 16.9522 (12)
β (°)	90.761 (1)
V (Å^3)	1560.4 (2)
Z	4
Radiation type	Mo $K\alpha$
μ (mm^{-1})	1.30
Crystal size (mm)	0.48 × 0.42 × 0.40
Data collection	
Diffractometer	CCD area detector
Absorption correction	Multi-scan *SADABS*
T_{min}, T_{max}	0.575, 0.625
No. of measured, independent and observed [$I > 2\sigma(I)$] reflections	7388, 2760, 2052
R_{int}	0.029
$(\sin \theta/\lambda)_{max}$ (Å^{-1})	0.595
Refinement	
$R[F^2 > 2\sigma(F^2)]$, $wR(F^2)$, S	0.035, 0.092, 1.06
No. of reflections	2760
No. of parameters	173
H-atom treatment	H-atom parameters constrained
$\Delta\rho_{max}$, $\Delta\rho_{min}$ (e Å^{-3})	0.26, −0.37

Computer programs: *SHELXL2018*/3 (Sheldrick, 2018).

Table 2

Hydrogen-bond geometry (Å, °) for (1884671)

D—H···A	D—H	H···A	D···A	D—H···A
N2—H2···Cl2^{i}	0.98	2.39	3.364 (2)	175

Symmetry code: (i) $-x, -y, -z+2$.

References

NOT FOUND

6. NMR spectrum of $L2_H$ ligand deprotonated by $AlMe_3$

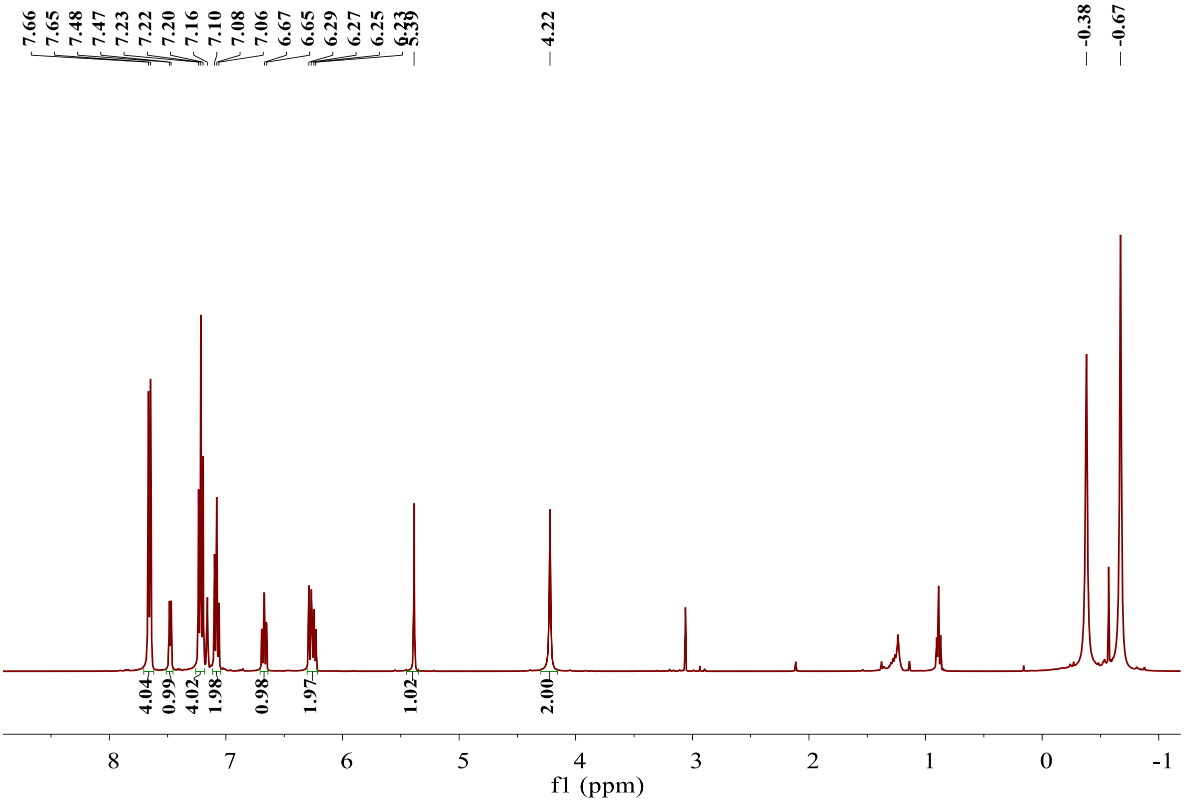

Figure S51 ^{1}H NMR spectrum (400 MHz, C_6D_6, 298 K)

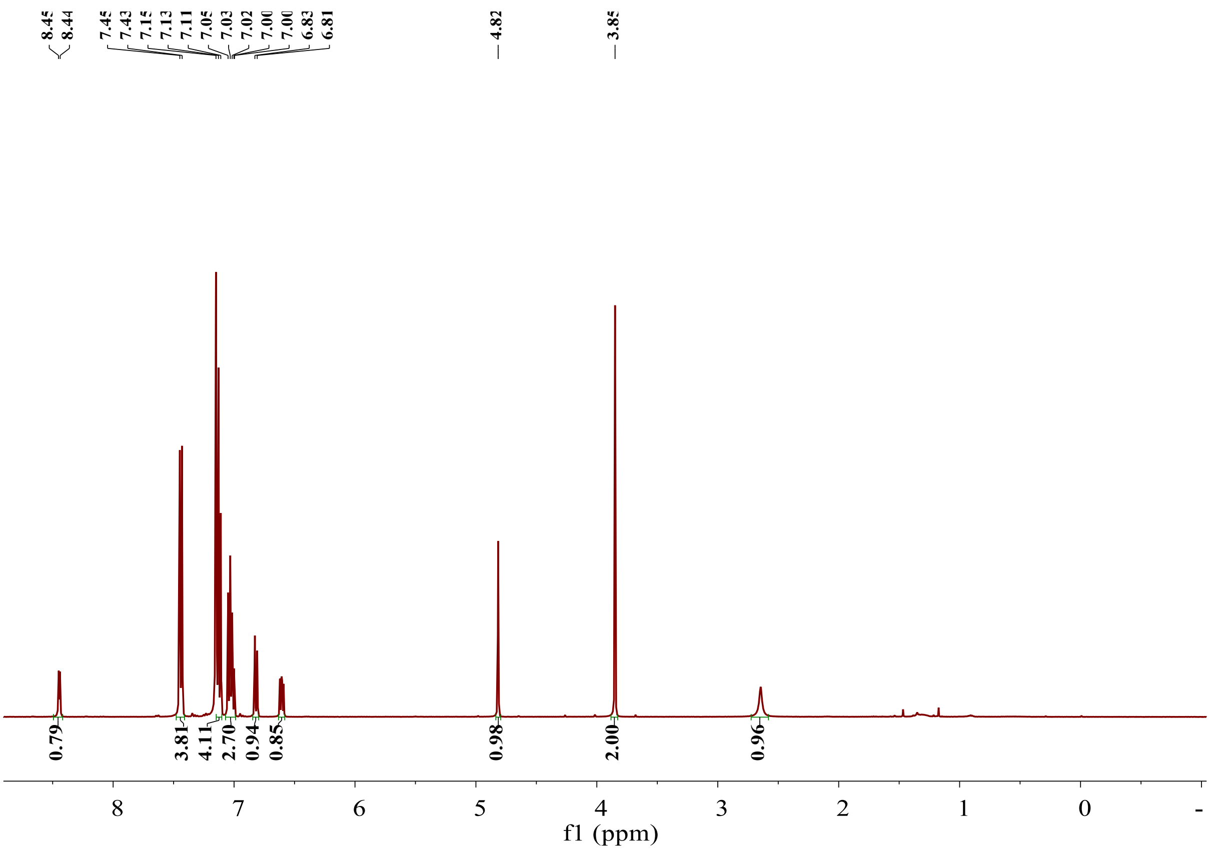

Figure S52. ^{1}H NMR spectrum (400 MHz, C_6D_6, 298 K) of $L2_H$